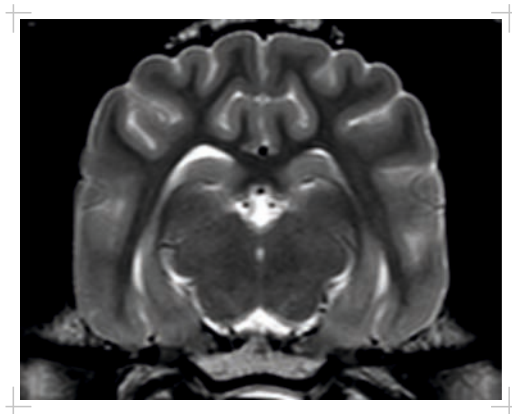


AGNIESZKA OLSZEWSKA

Interictal single-voxel ^1H -proton magnetic resonance spectroscopy of the temporal lobe
in dogs with idiopathic epilepsy



Inaugural-Dissertation zur Erlangung des Grades eines
Dr. med. vet.
beim Fachbereich Veterinärmedizin der Justus-Liebig-Universität Gießen

Das Werk ist in allen seinen Teilen urheberrechtlich geschützt.

Die rechtliche Verantwortung für den gesamten Inhalt dieses Buches liegt ausschließlich bei den Autoren dieses Werkes.

Jede Verwertung ist ohne schriftliche Zustimmung der Autoren oder des Verlages unzulässig. Das gilt insbesondere für Vervielfältigungen, Übersetzungen, Mikroverfilmungen und die Einspeicherung in und Verarbeitung durch elektronische Systeme.

1. Auflage 2019

All rights reserved. No part of this publication may be reproduced, stored in a retrieval system, or transmitted, in any form or by any means, electronic, mechanical, photocopying, recording, or otherwise, without the prior written permission of the Authors or the Publisher.

1st Edition 2019

© 2019 by VVB LAUFERSWEILER VERLAG, Giessen
Printed in Germany



édition scientifique
VVB LAUFERSWEILER VERLAG

STAUFENBERGRING 15, 35396 GIESSEN, GERMANY
Tel: 0641-5599888 Fax: 0641-5599890
email: redaktion@doktorverlag.de

www.doktorverlag.de

Aus dem Klinikum Veterinärmedizin
Klinik für Kleintiere, Chirurgie,
Neurologie und Neurochirurgie
der Justus-Liebig-Universität Gießen

Betreuer: Prof. Dr. Martin J. Schmidt

**Interictal single-voxel ^1H -proton magnetic
resonance spectroscopy of the temporal lobe
in dogs with idiopathic epilepsy**

INAUGURAL-DISSERTATION

zur Erlangung des Grades eines
Dr. med. vet.

beim Fachbereich Veterinärmedizin
der Justus-Liebig-Universität Gießen

eingereicht von

Agnieszka Olszewska

Tierärztin aus Olsztyn (Polen)

Gießen 2019

Mit Genehmigung des Fachbereichs Veterinärmedizin
der Justus-Liebig-Universität Gießen

Dekan:

Prof. Dr. Dr. h.c. M. Kramer

Gutachter:

Prof. Dr. Martin J. Schmidt

Prof. Dr. Michael Röcken

Prof. Dr. Joachim Roth

Tag der Disputation: 21.02.2019

To my Mom and Dad

Contents

- Abbreviations 7
- List of figures..... 10
- 1.Introduction 14
- 2. Literature review 15
 - 2.1 Definition of primary epilepsy 15
 - 2.2 Breed predisposition in idiopathic epilepsy 16
 - 2.3 Pathophysiology of primary epilepsy 17
 - 2.4 Morphology of the hippocampus 18
 - 2.5 The role of the hippocampus in epilepsy 24
 - 2.6 Refractory epilepsy 26
 - 2.7 MRI abnormalities in dogs with seizures 27
 - 2.8 Magnetic resonance spectroscopy 29
 - 2.8.1 Physical principles of MR-spectroscopy 29
 - 2.8.2 Quantification of MR Spectra 32
 - 2.8.3 Major metabolites 37
 - 2.8.3.1 N-acetyl aspartate (NAA) – the neuronal marker 38
 - 2.8.3.2 Choline (Cho) 42
 - 2.8.3.3 Creatine (Cr) 42
 - 2.8.4 Internal metabolite referencing 44
 - 2.8.5 MRS methodology on animal models of epileptogenesis 45
- 3.Research study 47
 - 3.1 Aim of the study 47
 - 3.2 Materials and Methods 47
 - 3.2.1 Study population 47
 - 3.2.2 Neurodiagnostic investigation 48

3.2.3 Anaesthesia protocol.....	49
3.2.3 Magnetic Resonance Imaging (MRI).....	49
3.2.4 Magnetic Resonance Spectroscopy (MRS)	49
3.2.6 Data processing and quantification	50
3.2.7 Statistical analysis.....	53
4.Results.....	54
4.1 Comparison of the metabolite ratios between the control and diseased group	61
4.2 Correlation between the metabolite ratios and the age and sex	63
4.3 Correlation between the metabolite ratios and the time from the last seizure in the group of the diseased dogs	65
5. Discussion.....	66
5.1 Limitations of the study	68
6. Conclusion	71
7. Summary.....	71
8. Zusammenfassung.....	71
9. Acknowledgments	72
8. References	73
9. Ethics	94

Abbreviations

¹H	hydrogen nucleus
¹HMRS	proton magnetic resonance spectroscopy
³¹P	phosphorus nucleus 31
AAT	aspartate aminotransferase
ADAM23	disintegrin and metalloprotease domain 23
ADC	apparent diffusion coefficient
AKG	alpha-ketoglutarate
ANOVA	analysis of variance
ANCOVA	analysis of covariance
Asp	aspartate
ASPA	aspartoacylase
Asp-NAT	aspartate N-acetyltransferase
ATP	adenosine triphosphate
CA	cornu ammonis
CA1	cornu ammonis field 1
CA2	cornu ammonis field 2
CA3	cornu ammonis field 3
CA4	cornu ammonis field 4
cAMP	cyclic adenosine monophosphate
CHESS	chemical shift selective method
Cho	choline
Cho/Cr	choline-to-creatine ratio
Cho/NAA	choline-to-N-acetylaspartate ratio
CK	creatine kinase
CK-B	brain-type creatine kinase
CL	citrate lyase
CNS	central nervous system
CoA	coenzyme A
Cr	creatine
CRT	creatine transporter

CS	citrate synthase
CSF	cerebrospinal fluid
CV	coefficient of variation
DV	dependent variable
Ento	cortex entorhinalis
EEG	electroencephalography
F	female
Fh	fimbria hippocampi
FLAIR	fluid-attenuated inversion recovery
FT	Fourier transformation
GABA	gamma-aminobutyric acid
Gde	gyrus dentatus
Glx	glutamate and glutamine peak
Glu	glutamate
GPC	glycerophosphocholine
LCModel	linear combination model
LG12	leucine-rich glioma-inactivated protein 2
M	male
Mal	malate
MM	macromolecules
MRI	magnetic resonance imaging
MRS	magnetic resonance spectroscopy
MRSI	magnetic resonance spectroscopy imaging
NAA	N-acetylaspartate
NAAG	N-acetylaspartylglutamate
NAA/Cho	N-acetylaspartate-to-choline ratio
NAA/Cr	N-acetylaspartate-to-creatine ratio

NMR	nuclear magnetic resonance
NP	number of phase-encoding steps
OAA	oxaloacetate
PC	phosphocholine
PCr	phosphocreatine
PDC	pyruvate dehydrogenase complex
PET	positron-emission tomography
ppm	parts per million
PRESS	point resolved spectroscopy sequence
SD	standard deviation
SE	spin echo
SE	standard error of the mean
STEAM	stimulated echo acquisition mode
Sub	subiculum
T1W	T1 weighted
T2W	T2 weighted
TCA	tricarboxylic acid
TE	echo time
TLE	temporal lobe epilepsy
TR	repetition time

List of figures

- Figure 1:** Anatomical structures of the hippocampal formation in the rat brain (Schmidt et al., 2015)..... 23
- Figure 2:** T2-weighted transverse MR-image of the brain formation of the healthy Beagle dog including the hippocampus within the temporal lobe (Images: © Martin Schmidt)..... 24
- Figure 3:** MR initial imaging study on a dog with generalised epileptic seizures (T2-weighted transverse and dorsal sequence (a-d)(i-l)) with unilateral hyperintense lesions at the level of hippocampus, similar to temporal lobe sclerosis, described in human medicine (Schmidt et al., 2015). 28
- Figure 4:** An example of a MRS spectrum obtained as a result of Fourier transformation, recorded at 3T with an echo time of 30ms (Barker et al., 2011)..... 31
- Figure 5:** Quantification of ^1H MR spectra as a linear combination of model spectra (LCModel)(Stagg et al., 2013)..... 33
- Figure 6:** The method of basis spectrum fitting. (Stagg et al., 2013)..... 35
- Figure 7:** Spectroscopic peaks of N-acetylaspartate (NAA), choline (Cho) and creatine (Cr) obtained with long echo time ^1H MRS of canine brain tissue at the level of posterior hippocampus and amygdala..... 37
- Figure 8:** NAA synthesis in the neuron (Moffett et al., 2013)..... 417
- Figure 9:** Metabolism of neuronal creatine..... 44
- Figure 10:** Transverse (A) and dorsal (B) T2-weighted MR images showing the position of point-resolved spectroscopy voxel ($10 \times 10 \times 10 \text{ mm}^3$)..... 50
- Figure 11:** Single spectrum from an individual voxel placed at the level of temporal lobe including a posterior part of hippocampus showing metabolite peaks of NAA at 2.0 ppm, Cr at 3.0 ppm, Cho at 3.2 ppm and the calculated

metabolite ratios in a mixed breed dog with degenerative disc disease included in the control group (A) and in 5 year old mixed breed male dog with idiopathic epilepsy and last seizure 5 days ago (B)..... 528

Figure 12: Distribution of epileptic convulsions in relation to time from last seizure in dogs from the study group. 56

Figure 13: Variations in metabolite mean values (NAA/Cr, Cho/Cr, NAA/Cho, Cho/NAA) between the control and epileptic dogs obtained in the region of the left and right temporal lobe including a posterior part of the hippocampus and amygdala. 60

Table 1: Number of different breed dogs comprised in the study group. Data included breed, sex, age in years and the time in days from the last seizure observed.54

Table 2: Dogs included in the control group. Data included breed predilection, sex, age and the diagnosis made based on the magnetic resonance examination.55

Table 3: Calculated metabolite ratios (NAA/Cr, Cho/Cr, NAA/Cho, Cho/NAA) obtained at the level of the posterior part of the hippocampus and amygdala for the left and right side of 27 dogs with idiopathic epilepsy included in the study group..... 56

Table 4: Calculated metabolite ratios (NAA/Cr, Cho/Cr, NAA/Cho, Cho/NAA) obtained at the level of the posterior part of the hippocampus and amygdala for the left and right side of 10 dogs included in the control group..... 58

Table 5: Mean, standard deviations, standard error of mean, coefficient of variation, biggest and smallest values for calculated brain metabolite ratios of canines included in the control and diseased group..... 61

Table 6: Comparison of the metabolite ratios (NAA/Cr, Cho/Cr, NAA/Cho, Cho/NAA) between the control and diseased group. The examined ratios for left and right region of interest similarly showed no significant difference between groups..... 62

- Table 7:** A three- factor analysis of covariance (ANCOVA) with repeated measure with respect to a side used to examine the correlation between the metabolite ratios and the age and sex of the diseased dogs. No significant differences in metabolite ratios were found when comparing healthy and diseased group regarding age and sex..... 63
- Table 8:** Significant positive correlation found between NAA/Cho ratio ($p= 0.03$) and Cho/NAA ratio ($p= 0.01$) and time from last seizure in comparison to the control group. Calculated regression coefficients show, how the metabolite ratio decreases (NAA/Cr, NAA/Cho) and increases (Cho/Cr, Cho/NAA) over time. Significant differences are highlighted in red..... 64

1. Introduction

Epilepsy is the most common neurological disorder in dogs (Kearsley-Fleet et al., 2013; Löscher, 1997; Thomas, 2010; Volk et al., 2015). It is characterized by recurrent seizures, which can have a focal or generalized semiology. Diagnosis and especially the management of the seizures remain challenging in some patients in veterinary neurology. It has been reported that over 30% of dogs are diagnosed with refractory epilepsy that does not sufficiently respond to anti-epileptic treatment (Martlé et al., 2014; Muñana et al., 2013). Surgical excision of the seizure focus is successfully performed in human patients with medically intractable epilepsy that arises from the hippocampus formation and associated structures with good long-term prognosis for seizure reduction, or even full resolution of seizures. Comparable surgical treatment for dogs with intractable epilepsy is not yet established, but could represent a promising option for the control of seizures in canine patients, too. Whereas the hippocampus has been clearly identified as a seizure generator in cats, the same evidence in dogs is less conclusive, and the morphology and function of the hippocampus in dogs with seizures is focus of intensive research. Some dogs present with atrophy or diffuse hyperintensities in the hippocampus, which suggest structural and functional changes in that brain area. These findings indicate some role in seizure pathogenesis. However, it remains unclear if the hippocampus is primarily changed (i.e. hippocampus sclerosis) or if the hippocampus underwent the same negative influences as the rest of the brain tissue after chronic seizure activity. Conventional magnetic resonance imaging (MRI) techniques are not always capable to visualize minor structural changes in the brain but also mostly cannot confirm, that the lesions observed in the sequences are in fact the underlying cause of the epileptic discharges. Magnetic resonance spectroscopy (MRS) is a non-invasive, in-vivo analytical technique obtained during standard MRI, which enables to observe the metabolic alterations in a specific region of interest in the brain. MRS is a relative new diagnostic tool in veterinary medicine and could be beneficial as a new evaluation method of the temporal lobe in epileptic dogs. In order to differentiate primary from secondary changes, spectra of the dogs with idiopathic epilepsy and generalized tonic-clonic seizures must be characterized as a baseline for future comparison.

The purpose of this prospective study was to evaluate the spectra of the common metabolites in the temporal region in dogs with non-lesional idiopathic generalised epilepsy using proton magnetic resonance spectroscopy (¹H MRS).

2. Literature review

2.1 Definition of primary epilepsy

Epilepsy is defined as a sudden, transient and abnormal phenomenon of a sensory, motor, autonomic, or psychic nature resulting from a transient brain dysfunction (Lorenz et al., 2011). The seizure can be caused by a secondary disease such as CNS infection, neoplastic disorders, intoxication or metabolic imbalances that all influence the membrane potential of the neurons. In primary epilepsy, no visible brain pathology can be diagnosed, which is why it is also often synonymously termed as idiopathic epilepsy. Following this definition, idiopathic epilepsy is diagnosed by exclusion of all possible secondary causes, and, in addition, based on the signalment, the typical age of onset, lack of interictal neurological clinical signs (DeLahunta & Glass, 2009; Dewey & da Costa, 2016). Idiopathic epilepsy is often age dependent and most dogs with primary epilepsy experience the first seizure at the age of 6 months to 6 years (Lorenz et al., 2011). The peak age of onset is at 1-3 years. However, the strict time frame is increasingly a matter of debate as several studies on Labrador retriever and Beagle puppies described possible earlier onset of few months of age (DeLahunta & Glass, 2009; Lorenz et al., 2011). Nevertheless, compatible age together with a normal physical examination, normal neurological examination, and normal bloodwork including complete blood count, full chemistry panel with electrolytes, bile acid profile, and a urinalysis is one of the indicators for a presumptive diagnosis of idiopathic epilepsy.

2.2 Breed predisposition in idiopathic epilepsy

Several canine breeds have a high incidence of seizure episodes, such as the Beagle, Belgian Shepherd, Belgian Tervuren, Bernese mountain dog, British Alsatian, Border collie, Dachshund, English springer spaniel, Finnish Spitz, Golden retriever, Irish wolfhound, Greater Swiss Mountain dog, Keeshond, Labrador retriever, Petit Briquet Griffon Vend'een, Shetland sheepdog, Standard Poodle, and Vizsla. However, any purebred or mix-breed dog can be affected with idiopathic epilepsy (DeLahunta & Glass, 2009; Dewey & da Costa, 2016).

Recently, a couple of gene defects were identified in dogs with heritable seizures. A truncating mutation in LGI2 (Leucine-Rich Glioma-Inactivated Protein 2) gene causing a lower neuronal threshold in Lagotto Romagnolo breed has been recognised (Seppälä et al., 2011). LGI proteins have a role in a synaptic transmission and regulate the development of the glutamatergic synapses (Pakozdy et al., 2013). They are also a part of a synaptic protein complex of the voltage-gated potassium channels. Their malfunction enhances glutamatergic transmission and therefore, lowers seizure threshold. The same research group confirmed that homozygosity for a two-SNP haplotype within the ADAM23 gene conferred the highest risk for epilepsy in the Belgian Sheepdog (Seppälä et al., 2011). The product of this gene is also involved in a synaptic transmission. In the hippocampus, both ADAM and LGI proteins are widely distributed in the granule cells of the dentate gyrus and CA3 and CA1 pyramidal neurons (Kalachikov et al., 2002). Although a genetic origin could not be found in other forms of idiopathic epilepsy, it is likely that in most, if not all epileptic diseases in dogs a genetic defect will be identified eventually. As the epileptogenic effect of these defects is caused by altered synaptic transmission and proceeds on the ultrastructural level in one-, or possibly multiple brain areas, such epileptogenic foci are beyond the structural changes that might be seen in the MRI.

2.3 Pathophysiology of primary epilepsy

The exact underlying mechanisms of the epileptic seizures are not completely understood, although numerous studies helped to define the major processes responsible for pathological epileptic discharges (Chapman et al., 1998; Chen et al., 2007; Vezzani et al., 1999). There are several reasons for the hyperexcitability of the neurons including lack of the neuronal inhibiting mechanisms, imbalance between the excitatory and inhibitory neurotransmitters or abnormal structure of ion channels. Moreover, the epileptiform activity can be a result of all these mechanisms simultaneously. The so-called “seizure threshold” is described as a level of neuronal inhibition, which maintains the neurons in a balanced state. The uncontrolled discharges in population of neurons are triggered by the disturbance in the neuronal environment, causing disproportion in the seizure threshold followed by neuronal excitation (DeLahunta & Glass, 2009).

The neuronal environment in the brain tissue is kept stable by neurons, the neuronal lipoprotein cell membranes with ion channels, the accurate concentration of the electrolytes (sodium, chloride, potassium and calcium) and the neurotransmitters. The astrocytes play also an essential role in metabolizing many of the neurotransmitters via transmission of the metabolites and ions through the walls of the blood vessels (DeLahunta & Glass, 2009). One theory regarding the insufficient inhibition of the brain activity in the cerebral cortex refers to lacking amount of the principal inhibitory neurotransmitters including gamma-aminobutyric acid (GABA), glycine, taurine and norepinephrine (DeLahunta & Glass, 2009; Dewey & da Costa, 2016). In the physiological environment, GABA is released into the synapse, where is attached to its receptors and monitors the passage of chloride through the ion channels, increases the potassium conductance and decreases the calcium entry, which has a slow inhibitory effect and stops the depolarisation. Alterations in GABA-ergic function have been reported in both human and animal epilepsy studies (De Deyn et al., 1990; Podell, 1997). A reduced inhibition of GABA-ergic effect leads to epileptic seizures, while the improvement of the GABA-ergic inhibition reduces the epileptic discharges (Wong et al., 1982; De Deyn et al., 1990). The alteration in any of the mentioned mechanisms leads to imbalance in seizure threshold observed clinically as an epileptic seizure.

The neurons express the hyperactivity through the excessive electrical discharges or increased amount of excitatory neurotransmitters (aspartate, acetylcholine or glutamate), which lead to marked and prolonged depolarization (a paroxysmal depolarizing shift) of the group of neurons in a certain area (focal seizure) or in the whole cerebrum (generalised seizure). The excessive expression of glutamate can lead to neuronal loss and apoptosis by increasing intracellular calcium concentrations (Fountain et al., 1995; Olney et al., 1986;). This process results in neuronal damage or their dysfunction, in which specific neuronal populations, such as hippocampal neurons, display a selective vulnerability. A unique feature of the hippocampus is its capacity for neuroplasticity, which may account for its pronounced vulnerability to conditions as seizures. Neuroplasticity creates new synaptic connections, spreading and enhancing electrical activity.

2.4 Morphology of the hippocampus

The complex terminology of the hippocampus and its adjacent structures can be a challenge to understanding, further complicated by the differences between human and animal morphology. The term hippocampus was coined by ancient anatomists. Watching into of the lateral ventricle of human brains, they described a ridge of grey matter tissue, elevating from the ventricular floor, which resembled a sea horse lying upside down in the temporal horn. This impression can be explained by the unique shape of the human hippocampus, which considerably differs from that in other animals. The head of the sea horse was seen in the *uncus* (lat. hook), which is the rostral part of the hippocampus that bends where it merges with the parahippocampal gyrus. The thick head of the human hippocampus was described as the belly of the sea horse, the digitations at the surface of the hippocampus seen as the trunk rings of the animal (Spruston & Mcbain, 2007). The body of the human hippocampus swiftly tapers to the tail that winds around the thalamus as such as the animals would hold on a water plant. In domestic animals, the hippocampus neither has an uncus, nor digitations or lack a clearly distinct dorsal tapering into a tail. The two hippocampi rather have a uniform shape in their dorso-ventral course (Nickel et al., 2003). They lie on each side of the thalamus and rather resemble a pair of horns

on the head of a ram, which is why it was also referred to as the Ammon`s horn (Ram's horn) (Spruston & McBain, 2007).

The hippocampus develops from the caudo-medial part of the cortical hemisphere that has infolded towards the lateral ventricle into a specialized area of allocortex, which comprises of two components. This is the actual hippocampus (hippocampus proper). The infolding process creates the hippocampal sulcus (also called hippocampal fissure) that separates the hippocampus from the laterally adjacent parahippocampal gyrus. At the beginning of their development, the cortical primordia of hippocampus and dentate gyrus are continuous. Then cells of this infolding cortical field detach, migrate to the end of the hippocampal cortex layer, surround it in the shape of a semicircle forming the dentate gyrus (Nickel et al., 2003). Macroscopically and microscopically the dentate gyrus and the hippocampus form an interlocking connection with one another (Figure 1). In addition, the term “dentate gyrus” originates on the observation of the human brain. After removal of the occipital pole of the hemispheres, the external surface of the dentate gyrus can be seen. In contrast to the smooth parahippocampal gyrus, the surface of the dentate gyrus has indentations resembling a row of teeth (*lat.:* *dentes*), which has led to the name of this structure. This characteristic indentation is also not seen in domestic animals (Nickel et al., 2003).

Within the parahippocampal gyrus, allocortex and neocortex gradually merge by progressive alterations of the cytoarchitectonic composition of the hippocampus that runs first into the subiculum and then into the entorhinal cortex of the parahippocampal gyrus. The hippocampus (proper), the dentate gyrus, the subiculum and the entorhinal cortex are referred to as the hippocampal formation (Figure 2)(Jung et al., 2010; Uemura et al., 2015;).

2.4.1 Cytoarchitectonics of the hippocampus proper

In contrast to the six-layered isocortex of the forebrain, the architecture of the hippocampus and dentate gyrus is relatively simple. Each part consists of only one layer of neurons. The principle neuron type in the hippocampus is the pyramidal neuron, in the dentate gyrus, it is the granule neuron. Pyramidal neurons of the hippocampus have a large triangular cell body and two distinct dendritic “trees”,

emerging from the base, and from the apex of the soma (Lorente de No, 1934). The position of the cell bodies and the arrangement of their dendrites create the characteristic lamination of the hippocampus in sectional images. In Nissl stain, that highlights the cell bodies, the layers where the perikarya of cellular elements accumulate, forms the stratum pyramidale. The layer underneath the pyramidal cell layer is called the oriens layer (stratum oriens; latin: “oriēns” in this context means “originating”), which contains unmyelinated basal dendrites of the pyramidal cells and scattered cell bodies of inhibitory basket cells. The underlying layer that borders the ventricular surface of the hippocampus is the alveus (latin “alveus”: riverbed or channel). It is composed of the myelinated axons of the pyramidal cells.

The area above the pyramidal layer adjoining the hippocampal sulcus is the molecular layer containing mostly the unmyelinated apical dendrites of pyramidal cells. It looks homogenous in Nissl stains. Staining techniques that highlight Zinc in synaptic connections with dendrites allow the identification of three sublayers characterized by different connectivity. Directly above the pyramidal cell bodies the straight apical dendrites of the pyramidal cells can be seen in almost parallel orientation. This layer is called the radiant layer (stratum radiatum) as the arrangement of the fibers in this layer reminded Cajal of sunrays (Ramon y Cajal, 1893). The stratum radiatum contains septal and commissural fibers as well as schaffer collaterals. The next sublayer is the stratum lacunosum that contains incoming fibers from the entorhinal cortex (perforant path). The last layer is the actual molecular layer (stratum eumoleculare), that houses the arborizing apical dendrites of the pyramidal cells. The last two layers are often grouped together as the stratum lacunosum- moleculare (Amaral and Witter, 1989).

2.4.2 Longitudinal divisions of the hippocampus (cornu ammonis fields)

The layers of the hippocampus slightly differ in their arrangement in dependence of their position between the dentate gyrus and the subiculum. In the proximal aspect of the hippocampus Cajal identified another narrow zone just above the pyramidal cell layer and underneath the radiant layer. Due to the paucity of cells and fibers in this layer it doesn't stain as intense as the other layers and appears translucent in the histological slides, which is why it was denominated stratum lucidum (latin: the

bright layer). The stratum lucidum contains unmyelinated axons originating in the granule cells of the dentate gyrus. These axons form characteristic dense synaptic connections (boutons) with the dendrites of the pyramidal cells that produce thin branches named "thorny excrescences" (latin: *excrescēntia* = abnormal growths (Amaral et al., 1989). These excrescences give the dendrites an appearance that reminded Cajal of a mosscovered tree (Raymon y Cajal, 1893). He introduced the name "mossy fibers" for axons that connect with the excrescences of the pyramidal cells. The presence or absence of the pyramidal cells with excrescences was the basis for the earliest classification of subfields in the longitudinal extension of the hippocampus in the rat as "regio superior" and "regio inferior" (Ramon y Cajal, 1893). The two early subdivisions of Cajal were later further divided into four subfields based on pyramidal cell morphology. The term cornu ammonis was adopted in abbreviated form as CA (Cornu Ammonis) in naming the four subfields CA1-CA4. In rats, pyramidal cell bodies in CA1 are smaller than in the other subfields, have a triangular shape and tend to stain less intensely in Nissl preparations (Amaral et al., 1989; Lorente de No, 1934). In CA3, that contains the mossy fibers, the cell bodies are larger, take up more stain, and are quite densely packed to a narrow band of cells. CA2 is a sort of a boundary zone sharing features of CA1 and CA3. It does not contain mossy fibers, but pyramidal somata are large as in CA3. The CA2 field has been a matter of some controversy. Its boundaries to CA1 and CA3 are clear in rodent and human hippocampi, but its presence could not be proven with certainty in all mammalian species (Amaral et al., 1989).

CA4 is easy to visualize. It is a loose segment of cells arranged around the end of CA3 that links up with the granular cell layer of the dentate gyrus. Unlike other pyramidal cells, the somata of CA4 do not form a recognizable layer. They are scattered among intertwined mossy fibers in the hilar region underneath the granule cell layer. The cells in CA4 do not have the characteristical pyramidal morphology, but are rather multipolar or fusiform neurons or have polymorph morphology (Lorente de No, 1934). Due to the unclear developmental origin and clear classification of the cells, the term CA4 has been abandoned from the modern anatomical terminology and was replaced by the term "endfolium" (latin: terminal leaf) of CA3. The cells of the endfolium are enclosed within the granular cell layer of the dentate gyrus. This area between the two blades of the granule cell layer is described as the hilus of the dentate gyrus (latin "hilum": "small depression" or

“indentation”). Although actually different structures, the terms - hilus and endfolium are commonly used synonymously. Also the dendrites of CA4 are covered by abundant thorny excrescences where they form synapses with the axons coming from the granule cell layer of the dentate gyrus.

2.4.3 Cytoarchitectonics of the dentate gyrus (dentate fascia)

The structure of the gyrus dentatus is simpler than of the hippocampus. Three layers are visible in Nissl stains. The main cell layer contains somata of very small granular neurons (stratum granulosum, Latin “granulum”: grain). It is a densely packed layer, whose shape is position- and also markedly species-specific. In dorsal slices of the rat’s hippocampus, it is presented as a more or less compressed “C” in the ventral (temporal) part of the hippocampus formation and as a “V” or a “U” in the dorsal (septal) part (Amaral et al., 2007). The limb of the granular cell layer, which is bounded between the CA3- and the CA1 field, is referred to as the supra-pyramidal layer or supra-pyramidal “blade”. The transition point adjacent to the end-folium is the crest of the layer, merging into the infra-pyramidal blade sitting below the CA3 field. The granule neurons have a round to elliptical cell body, which is also smaller than the soma of the pyramidal cells, and give rise to axons forming only one cone-shaped tree of spiny apical dendrites (Amaral et al., 2007). The stratum that contains these dendrites is relatively cell free. It is again called molecular layer analogous to the hippocampus, which can also be divided into two sublayers based on their connectivity. The area adjacent to the hippocampal sulcus is the outer molecular layer that receives fibers from the entorhinal cortex. The inner layer adjacent to the stratum granulosum contains fibers coming from the septal area and the hippocampus of the contralateral side (inner molecular layer). In between the two blades is the third layer of the dentate gyrus, the polymorphic cell layer (syn. stratum plexiforme; Latin “plexiformis”: grid-like). It contains a variety of neuron types and intermixed abundant unmyelinated nerve fibers. It is now recognized that there is no clear cut difference or border between the pyramidal neurons of CA4 and the neurons of the polymorphic layer. They are now considered to be the same neuronal population. The neurons in the hilus are also called “mossy cells”, as they have analogous thorny excrescences on their dendrites as the neurons of CA3.

The dentate gyrus is one of three areas in the brain where neurogenesis occurs. Neuronal stem cells reside in a thin layer at the border between the granule- and polymorphic cell layer, which is called the subgranular zone. They provide a reservoir for the turnover and replacement of granular cells that are functionally integrated into the granular cell layer (Amaral et al., 2007). This process continues to occur throughout life and provides plasticity, which plays a crucial role in learning and memory.

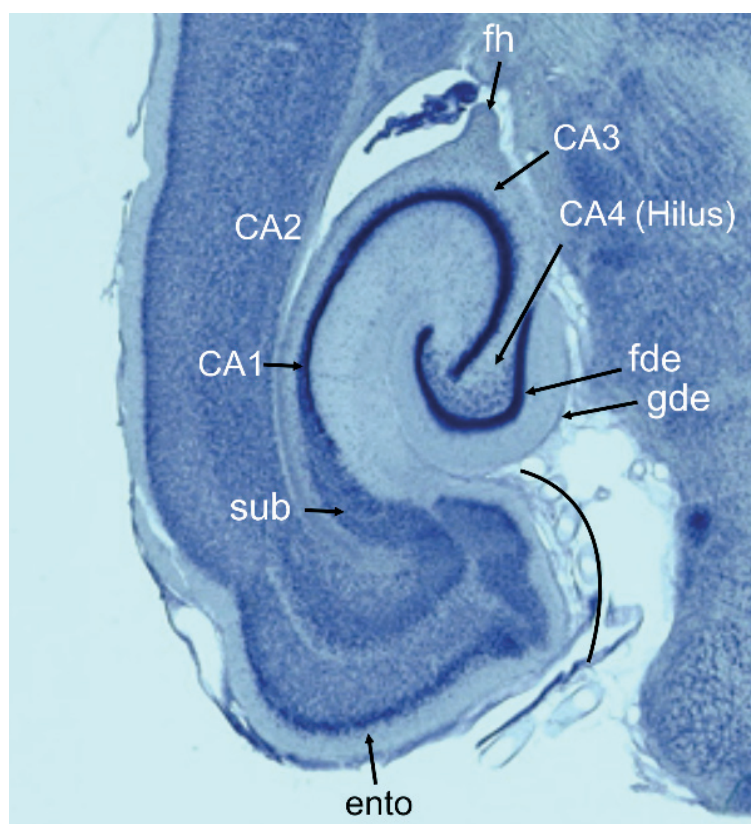


Figure 1: Anatomical structures of the hippocampal formation in the rat brain. CA1: cornu ammonis field 1; CA2: cornu ammonis field 2; CA3: cornu ammonis field 3; CA4: cornu ammonis field 4; ento: cortex entorhinalis; fh: fimbria hippocampi; gde: gyrus dentatus; sub: subiculum (Schmidt et al., 2015).

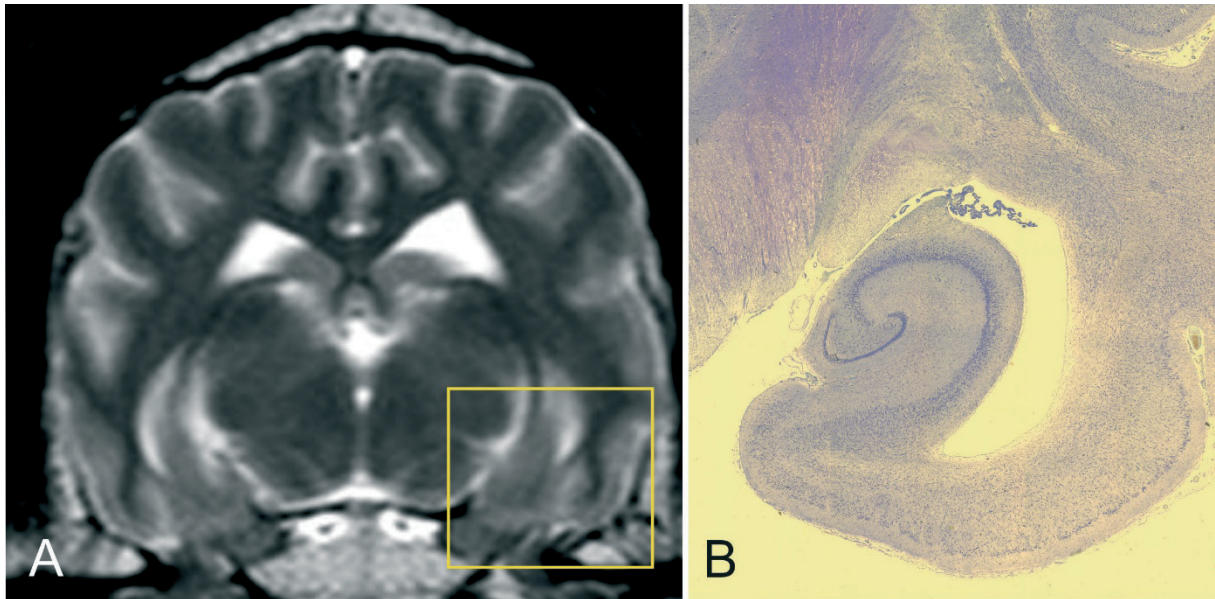


Figure 2: T2-weighted transverse MR-image of the brain formation of the healthy beagle dog including the hippocampal within the temporal lobe (A). The corresponding histological slide in Nissl staining (Chreysl-Violet) shows all structural elements of the temporal lobe in detail (B) (Images: © Martin Schmidt).

2.5 The role of the hippocampus in epilepsy

The hippocampal formation, entorhinal cortex and amygdala, situated in the temporal lobe, have been a subject of interest in both human and veterinary clinical and experimental medicine studies (Ben-Ari,1980 et al.; Calcagnotto et al., 2000; Jung et al., 2010; Löscher, 1997; Pakozdy et al., 2011; Spencer et al., 1992). "Hippocampal sclerosis" has been shown to be one of the most outstanding neuropathological findings, causing refractory epilepsy in human patients (Blümcke et al., 2009; Hauser et al., 1991). Hippocampal sclerosis is a result of the disorganisation of hippocampal cytoarchitecture, connectivity as well as gliotic atrophy of the pyramidal cell band of the cornu ammonis fields and in the hippocampus. It results in the deficit of almost 80% of the hilar somatostatin-immunoreactive inhibitory interneurons (Blümcke et al., 2002; Lanerolle et al., 1989; Mathern, 1995). The physiological role of the dentate gyrus is the transmission of the impulses that reach the hippocampus and further elaboration to the limbic cortices through the trisynaptic pathway (Behr et al., 1998). It undergoes structural remodelling of the dentate hippocampal circuits such as the loss of dentate hilus interneurons, presence of newly formed ectopic granule cells and mossy fibers

(Thom et al., 2009). Conversely, more recent papers suggest that the role of dentate gyrus is limited, showing similar hippocampal response in epileptic rats in comparison to control group (Ang et al., 2008).

Extensive studies on hippocampus and its function in epilepsy have been conducted in human medicine. However, up to date are only few case reports from veterinary medicine available. The neuronal damage has been described in dogs with prolonged seizures (Montgomery et al., 1983; Yamasaki et al., 1991). Nevertheless, neurons tend to be extremely vulnerable to excitotoxic injury due to long-lasting seizure activity, which could indicate only disturbances as a result of prolonged epileptic activity (status epilepticus), rather than hippocampal sclerotic changes. The occurrence of hippocampal sclerosis as an underlying cause for seizure activity in dogs remains controversial (Buckmaster et al., 2002; Koestner et al., 1989; Montgomery et al., 1983; Yamasaki et al., 1991). However, growing evidence suggests at least some role of the temporal lobe structures in canine epilepsy (Hasegawa, 2005; Schmidt et al., 2015). Hyperintense signals and atrophy of the hippocampus were demonstrated in MRI investigations of epileptic dogs (Kuwabara et al., 2010; Vullo et al., 1996) which is a sensitive and specific indicator of structural changes of the hippocampus in humans (Cendes et al., 1993; Cook et al., 1992; Jack et al., 1992). Furthermore, an increased apparent diffusion coefficient (ADC) was measured in the temporal lobe of epileptic dogs (Hartmann et al., 2017) which may be suggestive for underlying structural and/or functional abnormalities in this brain region. Experimental injection of kainic acid into the amygdala can produce complex partial seizures with associated rhythmic sharp waves in the left temporal region and bilateral volume loss of the temporal structures (Hasegawa et al., 2003). Finally, abnormal EEG activity, localized within the temporal lobe in dogs with natural occurring complex partial seizures could be found (Berendt et al., 1999) and was recently documented in association with hippocampal atrophy (Czerwik et al., 2018).

Even if the site of seizure onset is not in the hippocampus, it seems to be a route of propagation of the seizure discharge. In the epileptic hippocampus, the dentate gyrus undergoes changes including the loss of interneurons of the dentate hilus, appearance of ectopic granule cells, and sprouting of “mossy fibers” suggesting a remodelling of hippocampal circuits (Pitkänen et al., 2002). Cell death and loss of the CA1 network integrity can alter the responses of CA1 pyramids from

predominantly inhibitory to powerfully excitatory can, and thereby create a self-perpetuating loop that sustains seizure activity.

If seizure activity is enhanced in the hippocampus – primarily or secondarily – it might be a promising target for therapeutic strategies in veterinary medicine.

2.6 Refractory epilepsy

The term refractory epilepsy is used in veterinary medicine to describe the condition, where the patients do not respond to treatment of two or more conventional antiepileptic drugs and suffer from frequent severe seizures. The pharmacoresistance occurs in approximately 20-30% of epileptic dogs (Lane et al., 1990). Furthermore, less than 50% successfully treated dogs remain entirely seizure-free without unacceptable medication-related side effects including sedation, ataxia, polydipsia, polyphagia, hepatotoxicity and bone marrow suppression (Sander et al., 1993).

The inadequately treated epilepsy in both human and veterinary patients tends to worsen over time. Proposed theories regarding refractoriness involve mirroring and kindling. Kindling is termed as the phenomenon in which the constantly generated seizures from the epileptic focus lengthen in duration and the behaviour of seizure is enhanced until a plateau is reached. This is due to the repeated stimulation of the previously non-hyperexcitable neurons, which turn into a group of hyperexcitable neurons within a cerebral hemisphere. Mirroring has a similar mechanism of action to kindling, but involves recruitment of neurons into the seizure focus from the opposite cerebral hemisphere via the corpus callosum (Bertram et al., 2007; Dewey & da Costa, 2016). These processes change the ability of the brain to limit seizures. The refractory cases are particularly difficult to manage, thus additional diagnostic and therapeutic approaches need to be developed in order to improve the patient's quality of life and to plan the first epilepsy surgeries in veterinary medicine.

2.7 MRI abnormalities in dogs with seizures

Magnetic resonance imaging technique is frequently used as a diagnostic tool for dogs with epilepsy. Next to the exclusion of structural or metabolic brain diseases, lesions attributed to seizure activity affecting different regions of the human and canine brain can be observed. The lesions are usually hyperintense on T2-weighted images (T2W), typically affecting the temporal and piriform lobes, hippocampus or cingulate gyri in the brain (Chan et al., 1996; Schmidt et al., 2015; Yaffe et al., 1995). As the hyperintensities are usually reversible and resolve between 10 to 16 weeks following seizures (Mellema et al., 1999) it is assumed, that they represent regional cytotoxic oedema due to regional ischemia, although degenerative histologic changes in neurons have also been described (Chan et al., 1996; Sloviter et al., 2008). In some cases, the observed changes are permanent and tend to worsen over time (uni- or bilateral ventriculomegaly secondary to hippocampal atrophy) and might be representing the hippocampal sclerosis (Figure 3) (Czerwik et al., 2018; Hartmann et al., 2017; Schmidt et al., 2015).

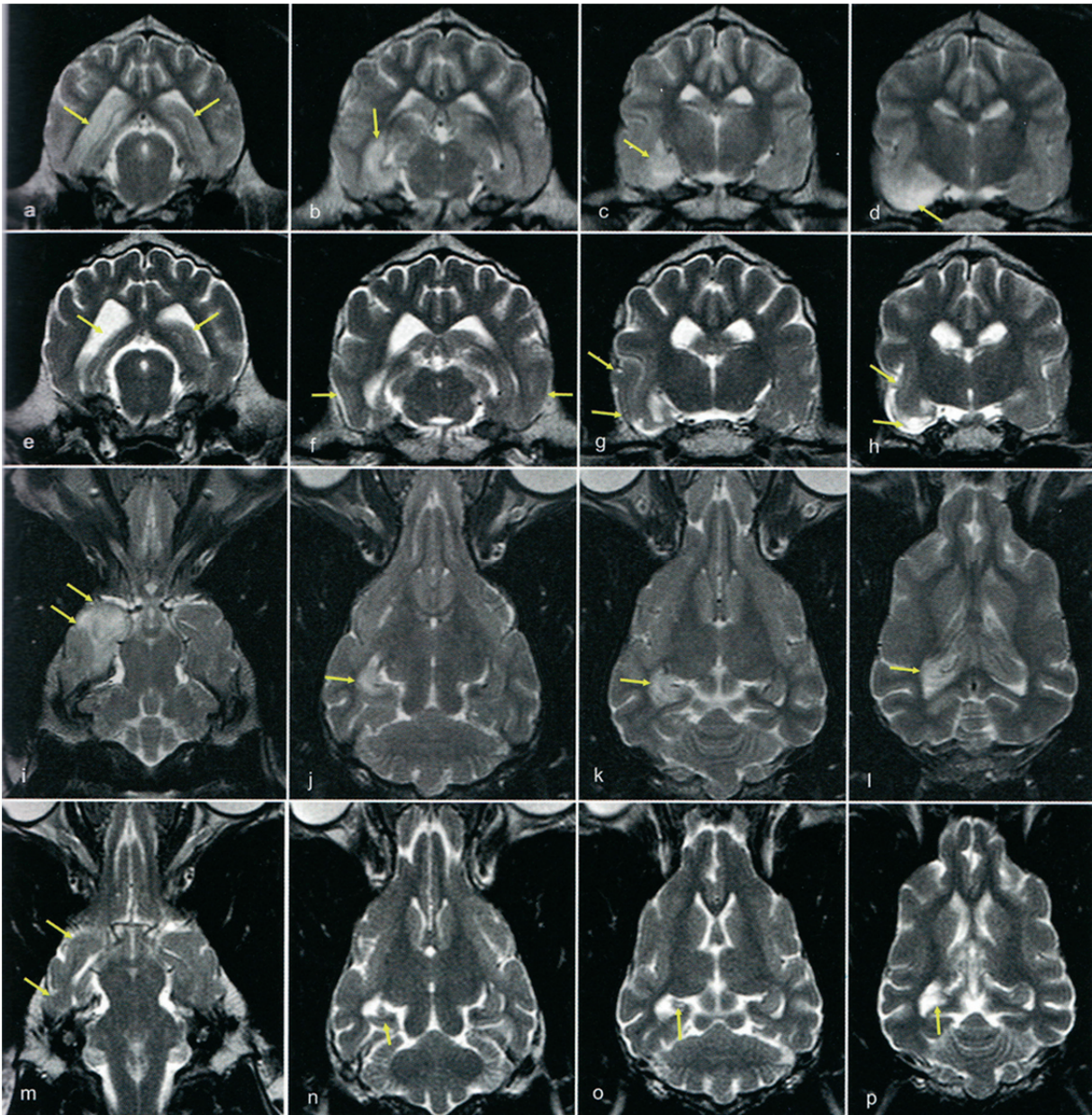


Figure 3: MR initial imaging study on a dog with generalised epileptic seizures (T2-weighted transverse and dorsal sequence (a-d) (i-l) with unilateral hyperintense lesions at the level of hippocampus, similar to temporal lobe sclerosis, described in human medicine. In the control study, ventriculomegaly secondary to hippocampal atrophy and hyperintensity at the level of cornu ammonis were observed (e-h) (m-p) (Schmidt et al., 2015).

2.8 Magnetic resonance spectroscopy

Magnetic resonance spectroscopy (MRS) is a unique diagnostic MRI technique, based on nuclear magnetic resonance (NMR) that allows quantitative *in vivo* assessment of concentration of metabolites in various tissues. It provides biochemical information about specific regions within the brain tissue of interest by detecting the resonance frequencies of metabolites. A quantitative evaluation of the specific substances with MRS can be used for differentiating several brain lesions, such as tumours, seizure-onset zone, strokes, inflammation, or oedema. It can be also applied as a tool to define brain maturation and aging. The first use of the proton MRS *in vivo* was reported by Behar, who examined rats at 8.5 T MRI, and the first spectra of metabolites including N-acetylaspartate, glutamine, glutamate, creatine, choline and lactate, were demonstrated in the rat brain (Behar et al., 1983). Magnetic resonance studies in laboratory animals for medical research as a model of human disease are performed with routine since then (Chatham et al., 2001; Hiremath et al., 2007; Nepl et al., 2001). The introduction of high field MRI in veterinary radiology and the improvement of acquisition and analysis techniques have also driven the evaluation of the technique for clinical studies in companion animals. Up to date available canine MRS studies include MRS spectrum analysis in hepatic encephalopathy (Carrera et al., 2014; Nyberg et al., 1998;) or tick-borne encephalitis (Sievert et al., 2016). Magnetic resonance spectroscopy have also been used as a monitoring treatment tool in dogs with meningoencephalitis of unknown origin (Beckmann et al., 2015). Recently data on ¹H MRS of the brain of healthy beagles have been reported and the differences in regional metabolite concentrations have been demonstrated using 3 Tesla and 7 Tesla MRI (Ober et al., 2013; Ono et al., 2014; Martin-Vaquero et al., 2012). Other than these studies, MRS is a technique in its infancy in veterinary medicine.

2.8.1 Physical principles of MR-spectroscopy

The physical mechanism of magnetic resonance imaging is based on the absorption of electromagnetic waves by the non-zero spin atomic nuclei (e.g. ¹H, ³¹P). Most MRI studies have been performed using the hydrogen nucleus ¹H due to its high

sensitivity to bound in tissue water which provides also the basis for MR imaging, so the hardware can be obtained for both techniques simultaneously. Hydrogen is also dominant in the most metabolites in the brain tissue. Other nuclei (phosphorus-31, carbon-13, nitrogen-15) are rarely used because of the lower sensitivity, worse special resolution and natural abundance in comparison to hydrogen which prolongs the scan time and enlarges the voxel size (Barker et al., 2011).

The absorbed electromagnetic waves are stored as energy and then returned in the process of relaxation during recovery of the spins to thermodynamic balance. Nuclear spins behave in the magnetic field like magnets that become polarized parallel or antiparallel. Energy radiated by these nuclei, after applying the radiofrequency electromagnetic waves typical for individual chemical compounds, is absorbed by spins in a magnet, which transform from the antiparallel to the parallel state and could be detected by the MR spectrometer in MRI receiving coil (Barker et al., 2011; Stagg et al., 2013). This resonant phenomenon and the resulting emitted radiofrequency signal is the essential principle of NMR.

In order to obtain good quality spectra, magnet field of 1.5 to 7 T in field strength should be used. The lower field scanners are disadvantageous due to lower sensitivity, which arises from the proportion of energy per absorption and emission to frequency. The quality of the NMR spectrum increases linearly with increasing the strength of field (Stagg et al., 2013).

A series of substances that play an important role in neurotransmission and brain energetics can be detected by MRS in vivo. Unfortunately, the majority of metabolites have concentrations below the millimolar detection limit. Nucleus' MR frequency of metabolites during screening is termed as chemical shift and stands for the main concept of MRS. ^1H chemical shifts acquired in vivo are valued as differences of parts per million (ppm). These compounds can be distinguished from each other and seen as characteristic peaks at different frequencies on the x-axis of the spectrum (Stagg et al., 2013). All the resonances of the metabolites are collected concurrently in the time domain, which makes it impossible to interpret for a human eye.

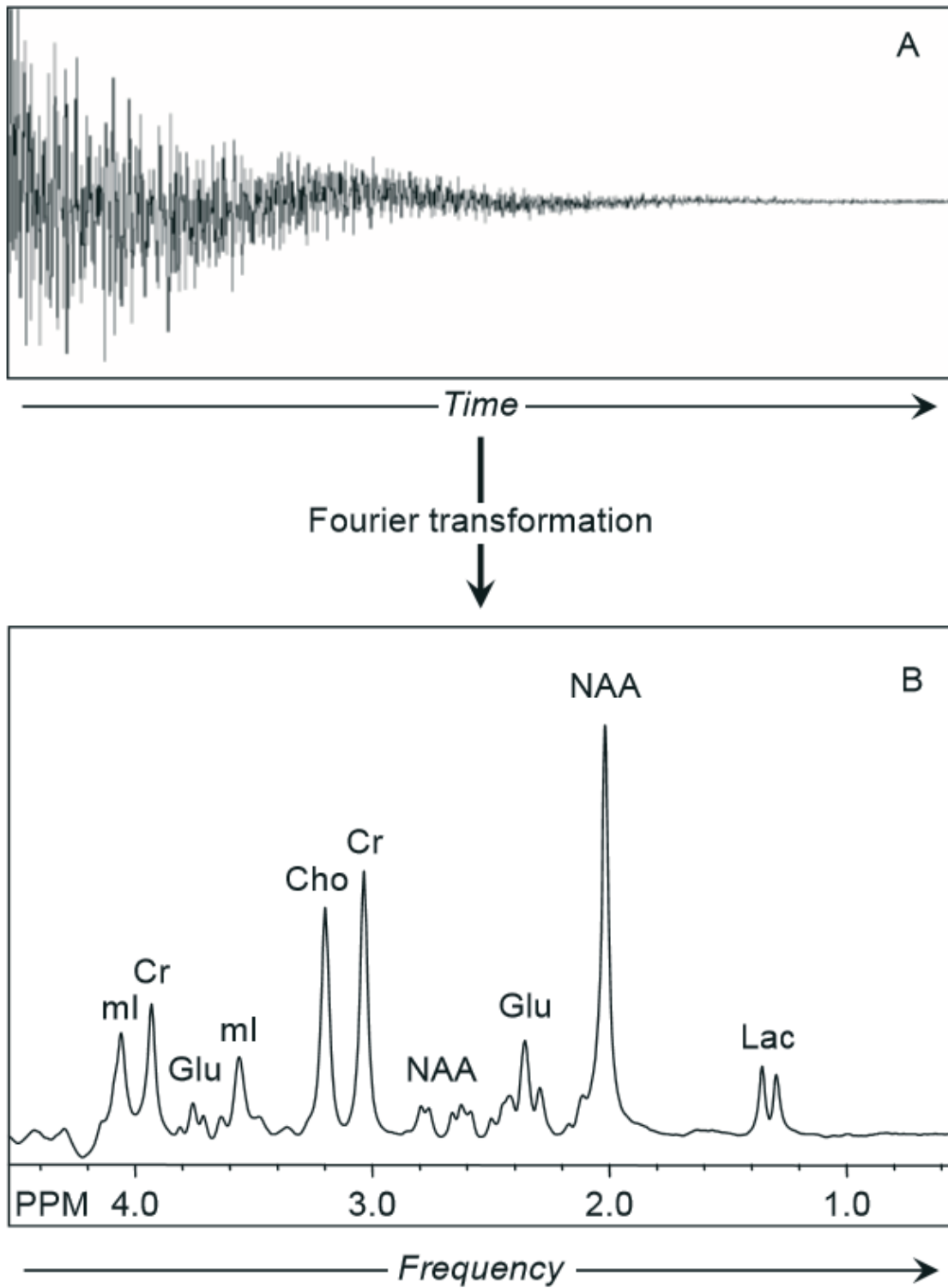


Figure 4: An example of a MRS spectrum obtained as a result of Fourier transformation, recorded at 3T with an echo time of 30ms (Barker et al., 2011).

The method called Fourier transformation (FT) needs to be obtained, so that the actual spectrum can be generated. Fourier transformation converts the signal intensity from time domain into frequency domain. It allows acquiring all signals of the metabolites in the field of interest at once. Because the Fourier transformation is a form of Gaussian fitting itself, this model is used most broadly due to obtaining the sharpest- shaped peaks in the frequency domain (Figure 4)(Stagg et al., 2013).

2.8.2 Quantification of MR Spectra

The aim of the MRS is the non-invasive quantification of the chemical compounds in the field of interest in the brain. However, the spectra acquired from a desired area of the brain contain the combined information from all distinguished metabolites as sum of their particular concentrations. Moreover, a number of additional, unwanted signals from sources other than the brain metabolites such as lipids, water and other macromolecules are visible in the acquisition and have to be taken into account when obtaining the MRS data. The spectra are also dependant on the technique that is used to obtain them, including the strength of field and a choice of echo time for the examination. Therefore, different methods of quantification and the same parameters need to be acquired in order to get reliable results. The most popular quantification method is a linear combination of model (LCModel). After the necessary scaling, the area under each peak is proportional to the number of protons with resonance frequency, which allows the evaluation of the relative concentrations of known substances. For each metabolite, the obtained scaling links to an apparent concentration (Figure 5) (Stagg et al., 2013).

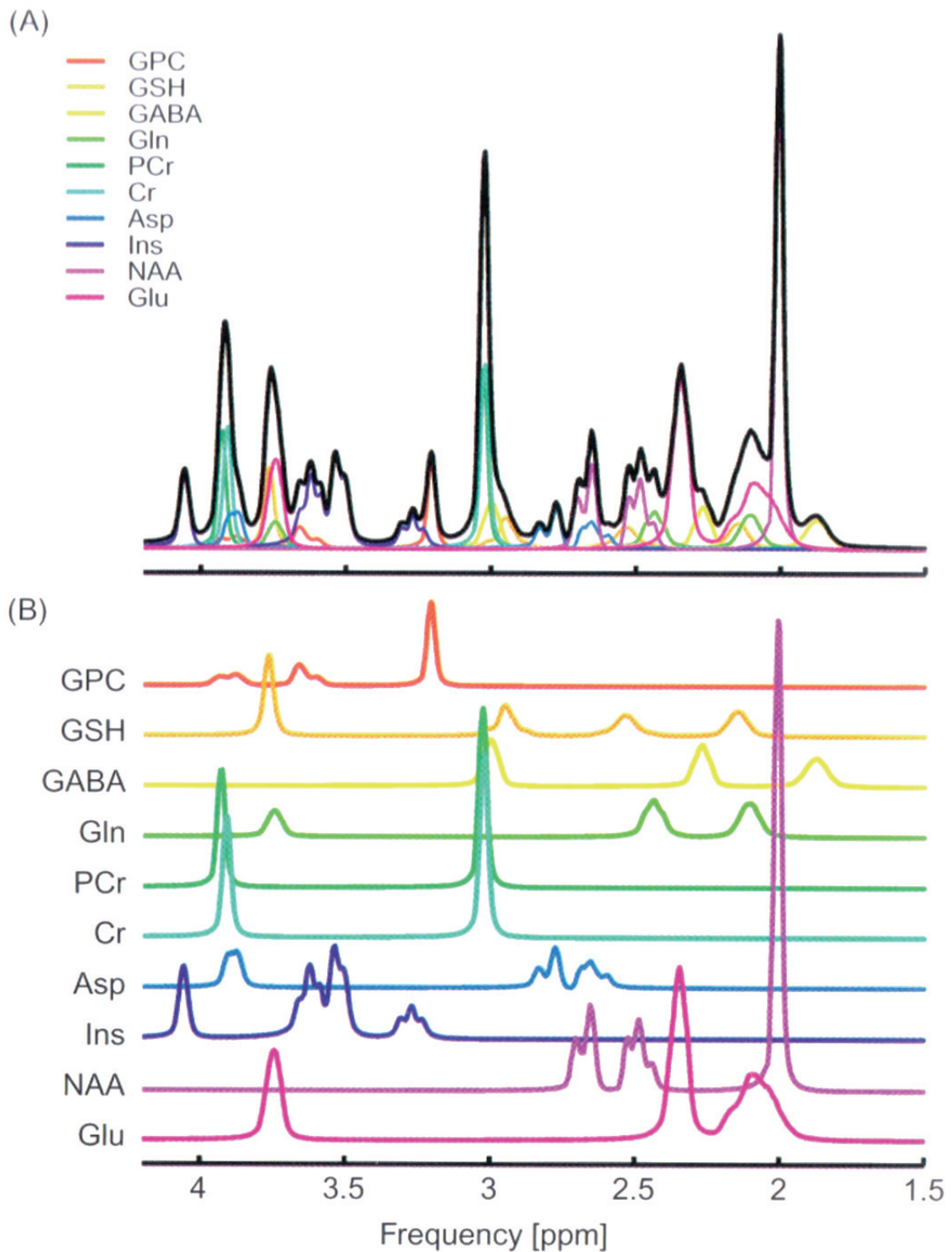


Figure 5: Quantification of ^1H MR spectra as a linear combination of model spectra (LCModel). (A) ^1H spectra comprise a sum of signals from the apparent neurochemical profile. (B) The spectrum contains a combination of the spectral patterns from individual metabolites. The necessary scaling corresponds to the apparent concentration of the substances. (Stagg et al., 2013).

The detection of the brain metabolites in brain tissue is challenging, as the concentrations are 10^3 - 10^4 times smaller in contrast to water molecules which dominate in volume, occupying around 70-80% of the grey and white matter. When the water peak remains unsuppressed, it overlaps all the relevant metabolites for the examination. For this reason, direct water suppression needs to be applied before, thus the metabolites signals can remain unaffected and water signal saturated.

Most of the metabolite peaks consist of over 10 individual peaks, so the total number of defined peaks would be too large to specify the precise value. Therefore, special fitting method called basis spectrum fitting is required in order to present an individual metabolite's spectral shape. This technique is usually proceeded automatically and involves fitting the entire spectrum as a linear combination of the basis spectra of all the molecules (Figure 6).

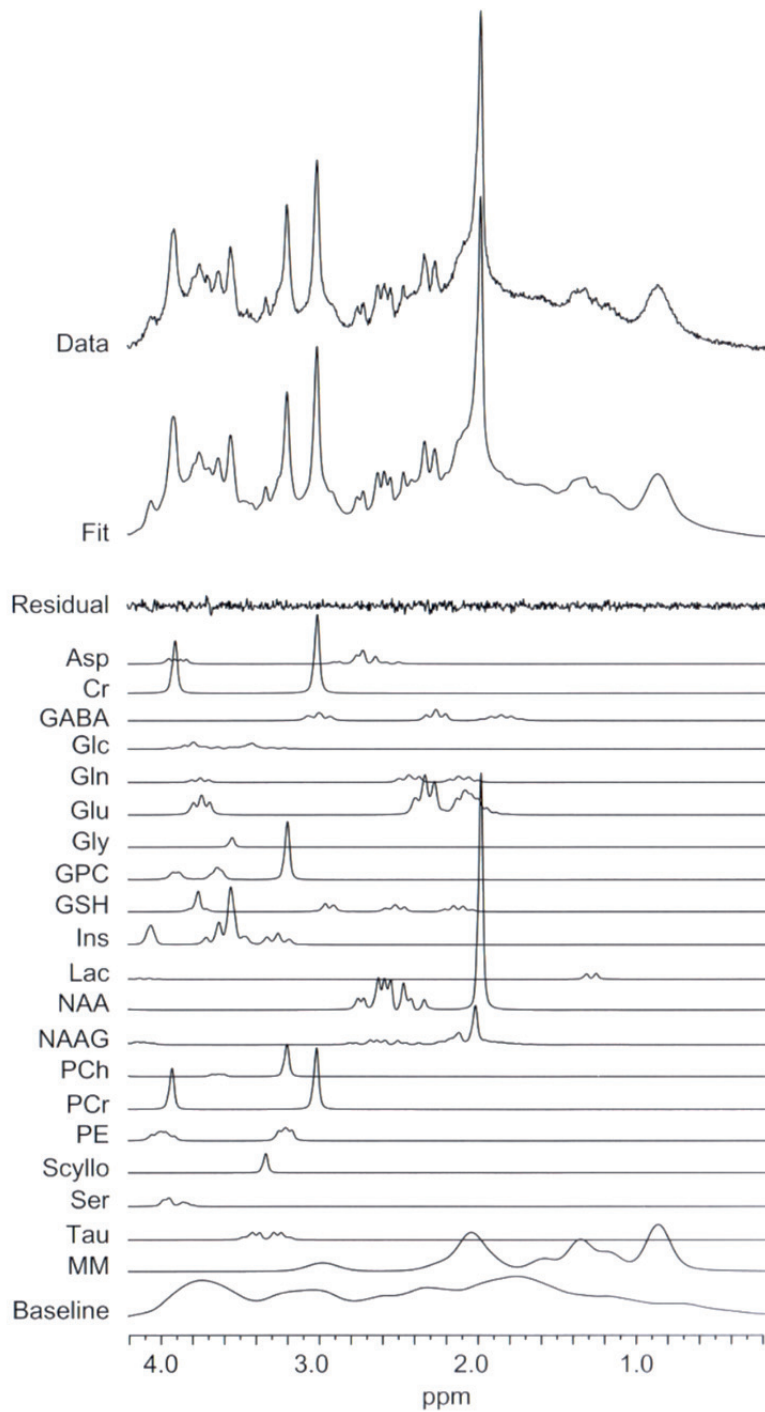


Figure 6: The method of basis spectrum fitting. The entire spectrum is fit to a linear combination of model spectra or basis spectra. Each basis spectrum corresponds to an individual metabolite, and the amplitude of the basis spectra represents the metabolite concentrations (Stagg et al., 2013).

The unwanted macromolecules can be simply separated from measured peaks by applying long echo time sequences where they are almost completely eliminated. Almost all macromolecules (MM) have short relaxation times (~250ms) which makes them invisible in comparison to other substances (NAA, Cr, Cho) that have $TE \sim 1500ms$ (Stagg et al., 2013).

Magnetic resonance spectroscopy can be proceeded in two different ways: single-voxel acquisition and multivoxel acquisition. With single voxel localization technique, a voxel (a volume of space) is applied in the tissue of interest and the proton signal in the voxel is used to produce a single spectrum. It is desirable to gain the information from a specific brain area due to extensive cellular heterogeneity. In practice, two pulse techniques are mostly used: Point Resolved Spectroscopy Sequence (PRESS) and Stimulated Echo Acquisition Mode (STEAM). The single-voxel technique is relatively easier to interpret and can be proceeded in shorter scanning time, as the signals from other brain regions are being isolated. The sensitivity to artefacts is also lower in comparison to multivoxel sequences. Single-voxel spectroscopy is a recommended approach to obtain the data in epileptic patients, that need to be scanned in the anaesthesia (Stagg et al., 2013).

Both techniques have been a subject of a constant comparison, nevertheless PRESS sequence is more frequent applied because of its relative insensitivity to motion and instability of the system. The multivoxel technique allows the definition of the multiple areas of the brain by applying numerous voxels in single sequence. The greatest limitation of this technique is relatively long examination due to combined acquisition, which prolongs the anaesthesia of the patient. The other limitation is the heterogeneity of the scanned tissue and some amount of signal obtained from outside the voxel area, which should be considered when obtaining the metabolite concentrations.

2.8.3 Major metabolites

The major brain metabolites analysed with long echo time ^1H MRS of brain tissue using 1.5 Tesla MRI include N-acetyl aspartate (NAA), choline (Cho) and creatine (Cr), as these have the most prominent and readily identifiable peaks (Figure 7). These three large singlet resonances dominate at long echo time times, because of T2-decay and scalar evolution, which makes it difficult to observe the other macromolecules (Stagg et al., 2013). Regional metabolite variations are observed both in human and veterinary patients (Carrera et al., 2014; Warrington et al., 2013), also change with brain development and aging (Chiu et al., 2014).

Other brain metabolites can be also estimated using MRS, however the accurate quantification is currently difficult due to the use of special sequences and particular echo time. These neurochemicals, currently described as nuisance signals, are glutamine, glutamate, lactate, lipids, myo-inositol, gamma-aminobutyric acid (GABA), alanine, and leucine.

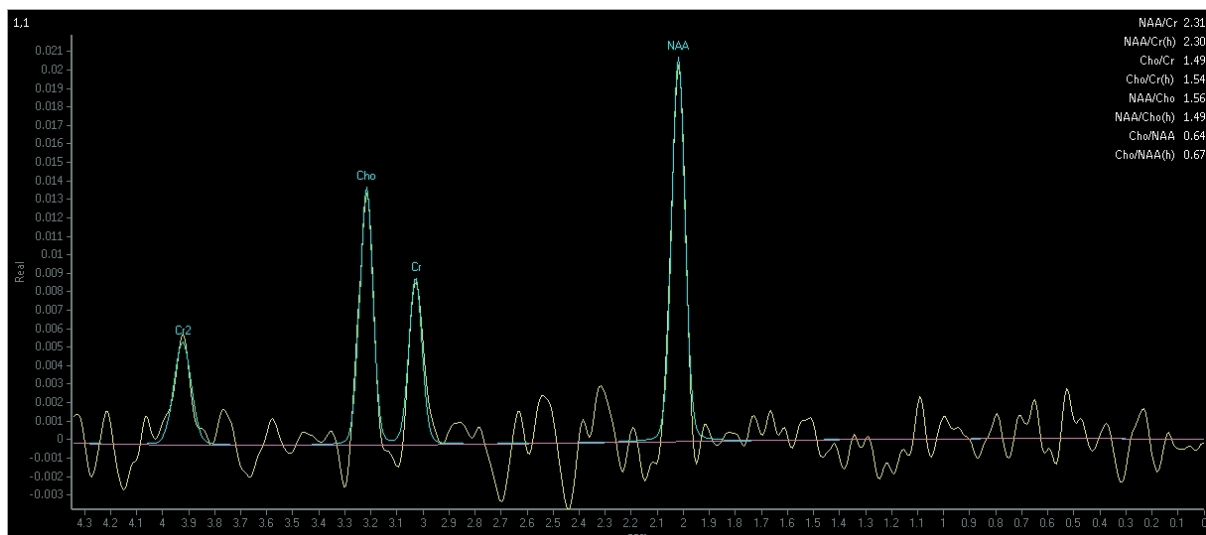


Figure 7: Spectroscopic peaks of N-acetyl aspartate (NAA), choline (Cho) and creatine (Cr) obtained with long echo time ^1H MRS of canine brain tissue at the level of posterior hippocampus and amygdala.

The increasing availability of new ultra-field scanners is promising to better investigate the clinical application of these markers in veterinary medicine. The peak intensity of the spectra alone is meaningless and presented in arbitrary units. This signal can be influenced by several parameters involving the placement and size of a voxel, coil sensitivity, type of the scanner the strength of field and receiver gain. The observed peak intensity needs to be transformed into a significant value by using the comparison to the metabolite reference peak, which is relatively stable in the examined tissue.

Spectral quantification is in principle a straightforward process. However, in the clinical use it is more problematic because of the presence of artefacts, complex spectral line shapes, overlapping peaks, different times, relaxations and macromolecule signal contaminations.

2.8.3.1 N-acetyl aspartate (NAA) – the neuronal marker

N-acetyl aspartate (NAA) stands for the most reliable marker of neuronal function and integrity and is considered one of the most abundant amino acids in the central nervous system. Other non-neural tissues have relatively small concentrations of NAA, below 40-50 μM (Miyake, 1981).

NAA it is referred to as a precursor for the biosynthesis of the neuronal peptide N-acetylaspartylglutamate (NAAG) and a marker of nerve cells in the nervous system (Figure 8)(Moffett et al., 2013; Stagg et al., 2013). However, the quantification of NAAG is more difficult because of a smaller size of a peak, which makes NAA the main interest of MRS studies.

The role of NAA in the brain is not fully recognised, it has been found in neurons, dendrites and axons during immunocytochemical staining techniques in a nervous system of humans, rats and cows, and dogs (Harris et al., 2006; Moffett et al., 1993; 1995; Nadler et al., 1972; Urenjak et al., 1992). The concentration was however undetectable in astrocytes and mature oligodendrocytes (Urenjak et al., 1992).

NAA signal peak is detected at 2.02 ppm and is more defined in contrary to the spectroscopic peaks of creatine and choline. It is believed that the level of NAA represents neuronal activity or neuronal loss in various neurological diseases (e.g. epilepsy, brain tumours, inflammation)(Hammen et al., 2012). It is not entirely

investigated whether the loss of NAA in the brain results from increased catabolism or decreased synthesis. In 1987, Hagenfeldt proved that NAA is catabolised by the enzyme called aspartoacylase (ASPA) in neurological disorders (Hagenfeldt et al., 1987).

N-acetyl aspartate was found decreased in various neurological diseases including epilepsy, presenting neuronal injury (Harris et al., 2006; Moreno et al., 2001; Riederer et al., 2006; Savic et al., 2000; 2004).

The concentration of N-acetylaspartate in neuronal mitochondria in the human brain was evaluated to be approximately 12mmol/L (Rigotti et al., 2007). In the rat brain the concentration ranges between 9.2- 9.3 mmol/L (Mlynarik et al., 2008). Recently, values for NAA concentration in a brain of healthy beagles were estimated ranging from 7.17 mmol/L to 7.90 mmol/L, depending on the brain region (Carrera et al., 2014). However, in a previous study on 10 healthy beagles, the mean NAA concentrations were at the level of 4,615 (Warrington et al., 2013). These concentrations varied significantly and were not normally distributed. To prevent measurement bias ratios of NAA-to-choline, mean of 1.294 (minimum 0.796 to maximum 2.318) and NAA-to-creatine, mean of 1.559 (minimum 1.145 to maximum 2.167) were proposed as a reference values (Warrington et al., 2013).

There are multiple theories about the actual function of NAA. It is responsible for supplying acetate groups for the synthesis of acetyl CoA (Burri et al., 1991; Mehta et al., 1995) and also involved in the synthesis of myelin and lipids in the CNS (Harris et al., 2006; Moffett et al., 2007).

The first reports on ¹HMRS in human patients with temporal lobe epilepsy showed a significant reduction of NAA in the hippocampus, suggesting temporary or permanent neuronal dysfunction in this area (Bernasconi et al., 2003; Simister et al., 2003).

MRS technique was similarly found valuable in lateralizing abnormalities regarding seizure onset in some patients with temporal lobe epilepsy, also in cases where the MRI was structurally normal. It was confirmed, that the metabolite abnormalities can occur uni- or bilaterally, mostly with significant reduction of NAA in comparison to control values (Aziz et al., 2016; Cendes et al., 1994; Connelly et al., 1994; Hetherington et al., 2007; Mueller et al., 2001). The bilateral changes of NAA can stand for a bilateral sclerosis or metabolic impairment as a result of the seizure in the epileptic side of the hippocampus propagating to the other side. This metabolic

disturbance represents rather a temporary dysfunction of neurons on the contralateral side and can improve over time after hippocampus surgery on the more affected side (Cendes et al., 1997; Vermathen et al., 2002). Even if in only small group of patients the epileptogenic focus was successfully lateralized, these patients had excellent surgical outcome (Kantarci et al., 2002).

NAA is a highly sensitive parameter. Its concentrations depend on the region, duration and therapeutic control of seizures. The NAA levels in a suspected epileptogenic region were found within the normal limits in patients with well controlled seizure activity. In patients, that did not respond to treatment or have not been treated so far, it was perceived that the NAA/Cr ratio can worsen over time, implying the progression of the hippocampus sclerosis or atrophy, whereas in successfully treated patients NAA level can improve over time suggesting rather reversible neuronal dysfunction than neuronal loss (Bernasconi et al., 2002; Hammen et al., 2012). Moreover, the lesions observed in MRI do not necessarily have to be involved in the aetiology of the epileptic seizure and show also normal levels of NAA (Kuzniecky et al., 1997).

N-acetylaspartate has been evaluated quantitatively as a concentration or as a ratio to creatine (NAA/Cr), as creatine believes to be a stabilization factor for many bioenergetic parameters and was found mostly in astrocytes. NAA/Cr ratio can be calculated with the purpose of presenting the neuronal metabolism and its dysfunction (Guevara et al., 2010; Maniega et al., 2008; Suhy et al., 2000). NAA/Cr ratio was also found relatively stable in a tissue containing cerebrospinal fluid, as it comprises only minimal amount of these metabolites. Spectroscopic abnormalities were found not only in a small area of hippocampus, occupying only some part of the temporal lobe, but also in the whole temporal lobe. These findings correlate with PET technique, and are due to the extensive hypometabolism in this area (Bernasconi et al., 2003; Simister et al., 2003).

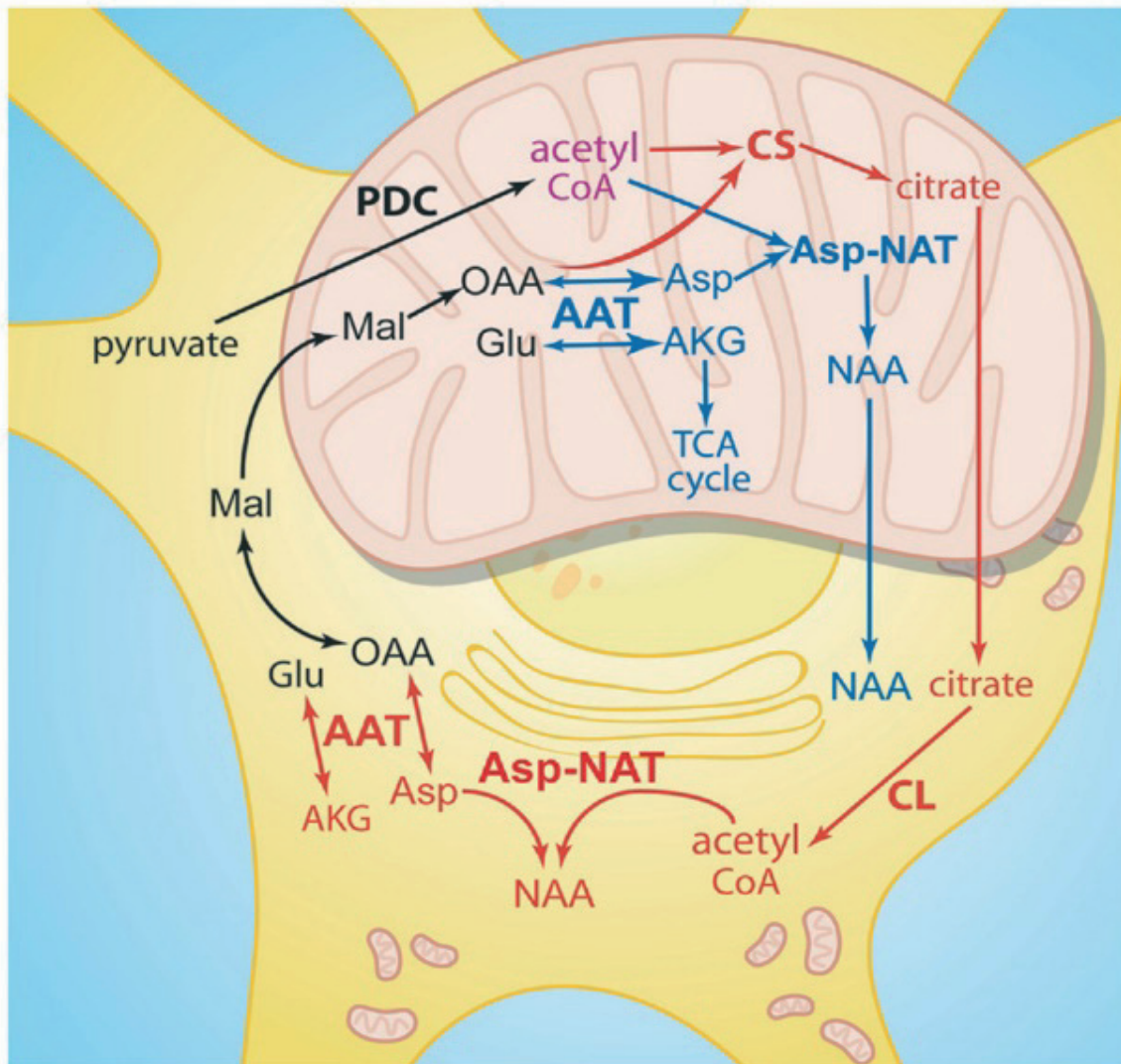


Figure 8: NAA synthesis in the neuron. Acetyl CoA derived from pyruvate in neuronal mitochondria can be oxidized for ATP production in the TCA cycle, or it can be utilized by two different enzyme pathways to produce metabolites for export to the cytoplasm. Acetyl CoA and oxaloacetate can be converted to citrate via citrate synthase (red pathway), or acetyl CoA and aspartate can be converted to NAA via Asp-NAT (blue pathway). NAA is also synthesized in the endoplasmic reticulum by cytoplasmic Asp-NAT using acetyl CoA derived from citrate. Citrate is then metabolized to acetyl CoA within the cell where it was synthesized, whereas NAA is predominantly transported to other cells such as oligodendrocytes for metabolism. AAT, aspartate aminotransferase; AKG, alpha-ketoglutarate; Asp, aspartate; Asp-NAT, aspartate N-acetyltransferase; CL, citrate lyase; CS, citrate synthase; Glu, glutamate; Mal, malate; OAA, oxaloacetate; PDC, pyruvate dehydrogenase complex (Moffett et al., 2013).

2.8.3.2 Choline (Cho)

Choline is an essential metabolite playing a complex function in the neuronal tissue. The main roles include the synthesis of cell membranes and its degeneration (membrane turnover). Moreover, Cho is a precursor of phosphocholine and acetylcholine and is involved in lipid transport and methyl- group metabolism (Loffelholz et al., 1993). Choline itself is absorbed from food, but also synthesized de novo and consequently bound in the phospholipids.

The signal peak of Choline (Cho), marked at 3.20 ppm is heterogeneous representing choline, phosphocholine (PC) and glycerophosphocholine (GPC) (Barker et al., 1994; Miller et al., 1996). The concentration of Cho represents cellular density and cell water turnover and it differs depending on the localisation. In the temporal lobe, the increased concentration level of choline is caused by accelerated phospholipid turnover and disruption in cellular membrane integrity in many neurological disturbances including neoplasia, ischemic injury and demyelination (Aziz et al., 2016; Farber et al., 1981; Van der Knaap et al., 2003). High concentration of choline has been found in glial cells. It may be also elevated in some diseases with active demyelinating process including multiple sclerosis (Arnold et al., 1992; Bitsch et al., 1999; Valenzuela et al., 2001). The changes in concentration can also be adaptive, suggesting the normalisation of the metabolic processes within time (Nordahl et al., 2005).

The mean choline concentration in the brain of the healthy dogs is 2.3 (± 0.17 mM) (Carrera et al., 2015). According to Warrington, the mean of choline-to-creatine ratio in 10 healthy beagles at an long echo time of 144 milliseconds was 1.240 (minimum 0.787, maximum 1.838) at the level of temporal lobe (Warrington et al., 2013).

2.8.3.3 Creatine (Cr)

Creatine in brain tissue is involved in transport, regulation and storage of cellular energy. Creatine is found in many metabolically active tissues including brain, heart and muscles. The appearance of Cr is both from endogenous synthesis and dietary products. Creatine plays essential role in energy synthesis being converted by creatine kinase (CK) to phosphocreatine (PCr) which is directly used in a production

of adenosine triphosphate (ATP) (Figure 9)(Stagg et al., 2013; Steen et al., 2010). Cr is supplied by creatine transporter (CRT) to the brain via blood-brain barrier (Braissant, et al., 2001). In adults, this mechanism is becoming insufficient within time, therefore an extra endogenous synthesis of Cr within the brain is used (Ohtsuki et al., 2002; Perasso et al., 2003). Cr is synthesized in axonal mitochondria, oligodendrocytes, dendrites, synapses and neuronal cell bodies.

The deficiency in Cr in a developing brain causes disturbance in axonal growth and axonal pathways plus reduced synaptic density which leads to mental retardation (Khwaja et al., 2008). In an adult brain, insufficient Cr synthesis and transport leads to deficiency in cellular energy homeostasis which causes mitochondrial dysfunction and further trigger to necrotic and apoptotic cell death (Desagher et al., 2000; Green et al., 1998; Roy et al., 2000). The clinical signs of this distortion include involuntary dyskinetic-dystonic movements, mental disability and epilepsy (Battini et al., 2002; Kleefstra et al., 2005; Mercimek et al., 2006; Rosenberg et al., 2004; Schulze et al., 1997; Stockler et al., 2007).

The creatine and phosphocreatine (Cr) is presented as a complex spectroscopic peak, observed at 3.03 parts per million (ppm). These two metabolite peaks overlap strongly on the spectrum and cannot be separated by any of the fitting methods.

Total creatine is often applied as an internal reference for MRS due to its relative stability in both normal and pathological brain tissue (Condon et al., 2011; Connett et al., 1988; De Stefano et al., 2002; Tartaglia et al., 2002). The concentration of Cr in dogs in the basal ganglia was found to be at 7.12 mmol/L in the left hemisphere, and 7.30 mmol/L in the right hemisphere (Carrera et al., 2015). The concentration of Cr in the cerebrospinal fluid has been proven to be negligible, therefore trace amount of CSF inside the applied voxel for the examination does not change the calculation of chosen metabolites (Hetherington et al., 1996).

Cr spectrum signal was also found significantly reduced in magnetic resonance spectroscopy in animal models of epilepsy (Hiremath et al., 2007) and in a canine model of PTY-induced generalized seizures (Neppl et al., 2001) and other human studies including stroke (Gideon et al., 1994; Lauriero et al., 1996; Lei et al., 2009; Mathews et al., 1995) and hyperammonemia (Braissant et al., 2002; 2010).

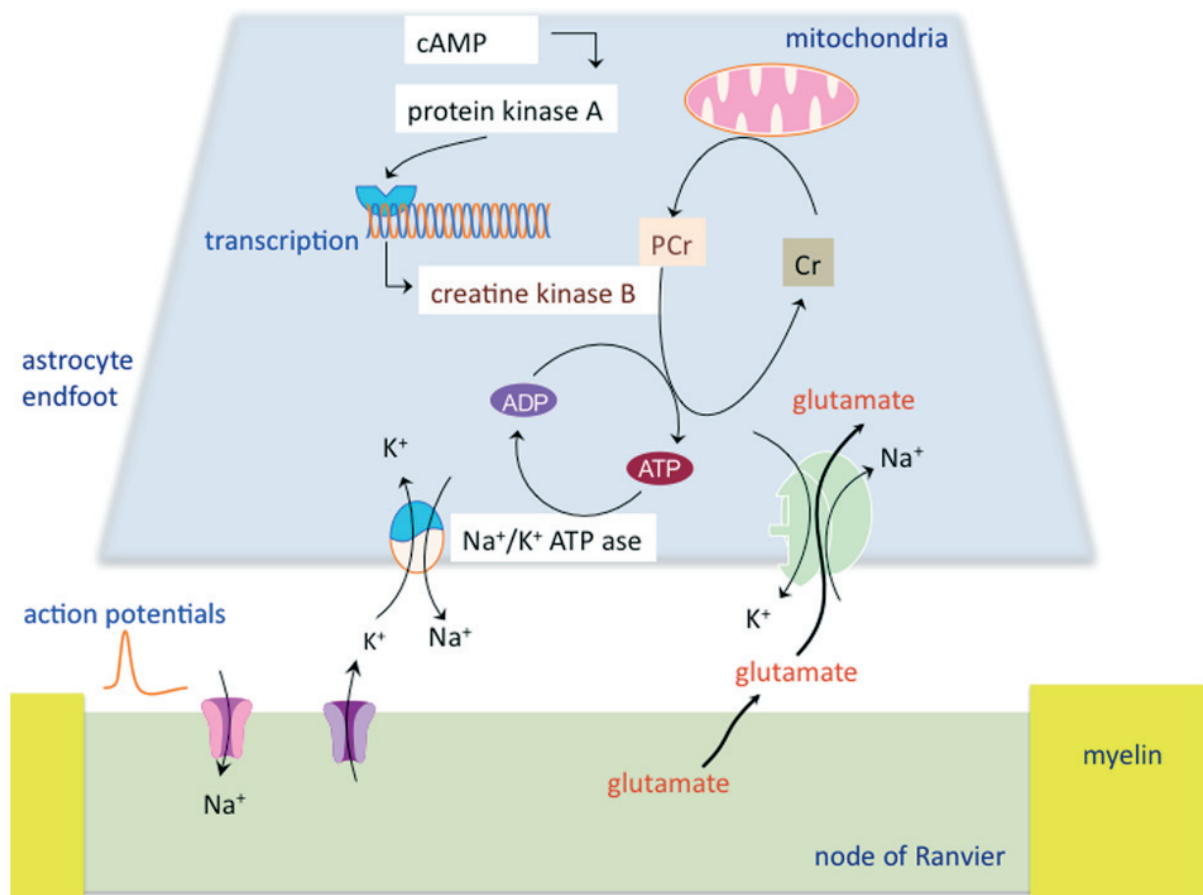


Figure 9: Metabolism of neuronal creatine.

Phosphocreatine (PCr) generated by mitochondria diffuses in the astrocytic processes where it is degraded by CK-B to deliver ATP. Creatine (Cr), formed by the removal of phosphate from PCr, diffuses into the mitochondria. This local energy is required for the Na⁺/K⁺-ATPase, which removes K⁺ generated during axonal electrogenesis from the extracellular space, and establishes the Na⁺ gradient required for Na⁺-dependent glutamate uptake by astrocytes. Transcription of CK-B appears to be mediated by cAMP (Steen et al., 2010).

2.8.4 Internal metabolite referencing

The absolute metabolite quantification can be obtained in different ways. One of the methods widely used is the acquisition of the resonance amplitudes as ratios rather than absolute concentrations, with the understanding that most factors affecting resonance amplitude are homologous for all metabolite resonances in the spectrum. This is because limited data on absolute quantification of metabolite concentrations is available and significant differences in absolute values varying significantly on the type of the scanner are presented in presented studies. Furthermore, several advanced spectral fitting techniques must be carried on in order to obtain relevant measurements.

The quantification of compounds is performed by comparison the metabolite of an interest (expressed in the numerator) with a reference metabolite (expressed in the denominator). The reference compound is chosen basing on its relative stability in the examined tissue. Creatine is often presented as a reference parameter because of high impact in bioenergetics and relatively stable value (Connett et al., 1988).

Mostly described metabolite concentration ratios include the NAA-to-choline, NAA-to-creatine, and choline-to-creatine ratios. The generally accepted values determined using ^1H MRS in the brain of healthy human patients are 1.6, 2.0, and 1.2, respectively (Alger et al., 2010). However, the latest studies in veterinary medicine presented that the comparison of the values to humans, assessed using ^1H MRS, should be done with caution due to significant differences in ratios between the healthy human and canine groups (Warrington et al., 2013). In latest veterinary studies, no significant differences in ratio values between the sexes and the hemispheres in the canine healthy brain were noticed (Carrera et al., 2015).

2.8.5 MRS methodology on animal models of epileptogenesis

MRS methodology for animal models in human brain diseases has been extensively studied in order to provide result for the clinical studies. MRS was first used as diagnostic tool for assessment of animal model of epilepsy on rats the early 1980s. In the performed studies on ^{31}P MRS it was first noticed, that status epilepticus is associated with the reduction of phosphocreatine (PCr) and occurrence of cerebral acidosis (Petroff et al., 1984). More recent studies on rats showed a significant decrease of NAA in both, the immediate days and chronically after status epilepticus that link with seizure-related injury (Hiremath et al., 2007; Filibian et al., 2012).

Preliminary results of a detection of postictal perturbances in cerebral metabolism in prolonged general seizures in 5 mixed-breed dogs using MRS at field strengths of 0.5 Tesla were described by Neppl (Neppl et al., 2001). Mean glutamine and glutamate (glx) concentration was significantly decreased in the postictal phase in these patients. Mean NAA concentration was not statistically significant in the mentioned study.

Magnetic resonance spectroscopy was proposed as a possible useful tool in diagnosing epileptic dogs (Condon et al., 2011; Rusbridge et al., 2015). To author's knowledge, no reports presenting use of magnetic resonance spectroscopy at field

strengths of 1.5 Tesla to evaluate regional differences in idiopathic epilepsy in dogs have been published up to date.

3. Research study

3.1 Aim of the study

The aim of our study was to evaluate the interictal metabolic activity of the temporal lobe region in dogs with idiopathic epilepsy and generalized tonic-clonic seizures using ^1H single voxel magnetic resonance spectroscopy compared to a group of clinically sound control dogs. We therefore describe the metabolite ratios obtained bilaterally, symmetrically at the level of temporal lobe and posterior part of hippocampus.

First, the calculated ratio values (NAA/Cr, Cho/Cr, NAA/Cho, Cho/NAA) are determined for healthy and epileptic dogs. This data was examined for a possible relationship between the metabolite ratios and the age and gender of the dogs. Second, values of the control group were compared to the epileptic dogs in the study group.

Finally, the correlation between the values of the metabolite ratios in patients with epileptic seizures and time from the last seizure are examined.

3.2 Materials and Methods

3.2.1 Study population

The study was a prospective, cross-sectional investigation. All the examined client-owned dogs were patients of the Department of Internal Diseases with a Clinic of Horses, Dogs and Cats of the Faculty of Veterinary Medicine, Wrocław University of Environmental and Life Sciences, Wrocław, Poland. All the owners signed a declaration of consent and information about the imaging study. Magnetic resonance examinations were carried out in the Center of Experimental Diagnostics and Innovative Biomedical Technologies, The Faculty of Veterinary Medicine, Wrocław University of Environmental and Life Sciences, Poland.

3.2.2 Neurodiagnostic investigation

The diagnosis of idiopathic epilepsy was based on clinical history of repeated seizures in dogs aged between 6 months and 6 years at the time of the first seizure onset, in which no known demonstrable genetic and pathologic cause has been found (DeLahunta & Glass, 2009). Clinical manifestation of epileptic seizures was documented by the owner on a video and could therefore be analysed by the investigators. The most frequent symptoms included jaw snapping, muscle rigidity, paddling of the legs, salivation, barking, jerking motions of the muscles, stiffening of the legs and neck and urination during or directly after the epileptic discharges. Some dogs showed aggression or change in the behaviour (tier I confidence level for the diagnosis of IE; De Risio et al., 2015). Cases suspected of paroxysmal events other than epileptic seizures, such as cardiogenic syncope, vestibular disease, narcolepsy, were excluded from the further study. The last epileptic seizure must have occurred within the last 4 weeks in order to investigate acute and subacute changes.

Complete clinical and neurological examinations were executed by a veterinary neurologist on all dogs from the control and study group. Following a routine protocol, pre-anesthetic laboratory investigations comprised complete blood cell count and serum biochemistry panel, electrolytes as well as fasted ammonia testing, and bile acids Cerebrospinal fluid (CSF) was obtained by puncture of the atlanto-occipital cistern with the dogs under general anaesthesia directly after the MRI examination. Cytologic and biochemical analysis of the cerebrospinal fluid including specific gravity, electrolytes, leukocyte count, complete blood count, protein concentration, Pandy's reaction, glucose were performed in all dogs. (tier II confidence level for the diagnosis of IE; De Risio et al., 2015). Ten dogs included in the control group went through a complete clinical and neurological examination. Complete blood count, biochemistry panel, cerebrospinal fluid examination and urinalysis was obtained in all dogs. They had no history of epileptic seizures. All dogs were presented for MR imaging for other clinical problems, mostly spinal cord abnormalities, and were aged between 1 to 4 years.

3.2.3 Anaesthesia protocol

All MRI and MRS were proceeded under premedication followed by general anaesthesia. Each patient underwent premedication using medetomidine (0,02 mg/kg i.m) and butorphanol (0.1 mg/kg i.m). The patients were intubated and positioned in a sternal recumbency. General anaesthesia was induced with Propofol (4-8 mg/kg i.v) and maintained by inhaled anaesthetics (1-3 Vol % Sevoflurane in oxygen).

3.2.3 Magnetic Resonance Imaging (MRI)

All MRI and MRS data were acquired in ventral recumbency with a high-field 1.5 Tesla MR scanner (Ingenia; Philips Medical Systems, 2013) using dStream HeadSpine coil (Philips Medical Systems, 2013). The following MRI pulse sequences were applied: 2 mm T2-weighted spin echo (SE) images, 2 mm fluid-attenuated inversion recovery (FLAIR) sequence, 0.8 mm T1- weighted 3D pre- and post- contrast images following intravenous administration of gadolinium (Gadobutrol 604.72 mg/mol). All MR sequences were performed as follows: conventional transverse and sagittal T2-weighted images (TR 4423.5 ms/ TE 100 ms), dorsal FLAIR (TR 9000ms/ TE 140 mg), 3D T1- weighted pre- and postcontrast images (TR 25ms/ TE 5.1 ms).

3.2.4 Magnetic Resonance Spectroscopy (MRS)

Single-voxel proton magnetic resonance spectroscopy was performed during the MRI study before intravenous administration of the contrast medium. The MRSI studies were targeted to suspected regions of interest (temporal lobe, hippocampal area) for seizure localization. A cubic voxel (10 x 10 x 10 mm³) was identical for all studies and positioned manually, bilaterally, symmetrically at thin, 2mm T2-weighted sagittal and transverse, 0.8 mm T1- weighted 3D pre- contrast dorsal into the region of left and right temporal lobe including a posterior part of hippocampus and amygdala (Figure 10).

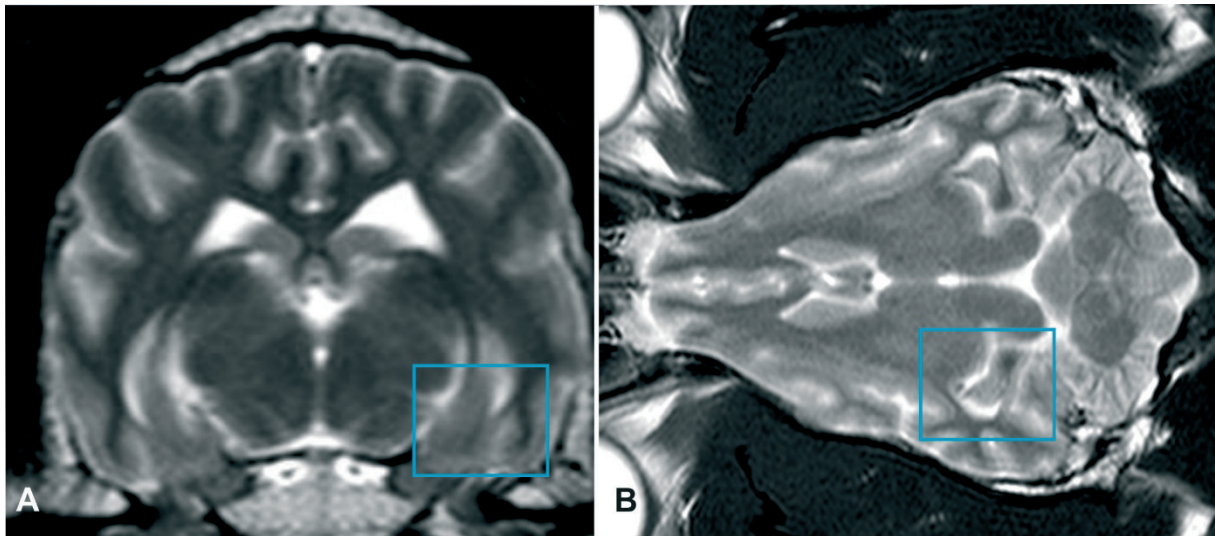


Figure 10: Transverse (A) and dorsal (B) T2-weighted MR images showing the position of point-resolved spectroscopy voxel ($10 \times 10 \times 10 \text{ mm}^3$) for the right side. The identical examination was performed for the left side.

The great caution was exercised when placing the voxel in order to prevent scalp fat and CSF contamination. The method of a point resolved spectroscopy sequence (PRESS) with chemical-shift selective (CHESS) pulse for water suppression (bandwidth 50 Hz) was obtained. The MRSI studies were acquired as Hahn spin echoes with repetition time [TR], 2000 milliseconds; echo time [TE], 144 milliseconds; the number of phase-encoding steps [NP], 1024. A total of 256 images were averaged for an acquisition time of 10 min for each investigated side of the mesial temporal/ hippocampal area. The accurate position of the voxel for each examination was controlled by the doctoral student (AO) and approved by the supervisor (MS).

3.2.6 Data processing and quantification

An automatic and operator-nondependent data processing system was used to obtain the spectra recorded for the analysis (SpectroView Analysis software, Philips Healthcare). The spectral post-processing included the adjustment of the base-line, the noise level reduction, and metabolite peak calibration, correction of the internal water referencing and the application of spectral plotting, followed by Fourier

transformation. Spectra were phased and fit in the spectral domain followed by Gaussian line-shaped transformation.

¹H MRS data with relatively unstable baseline despite post-processing techniques used suggesting either the involvement of the nuisance signals such as water, lipids or poor spatial localisation of the voxel, were excluded manually by doctoral student (AO) from further analysis. The following signals of metabolite peaks in the applied long echo time sequences were detected: N-acetylaspartate (NAA) at 2.02 ppm, choline (Cho) at 3.22 ppm and creatine (Cr) at 3.02 ppm. The NAA, Cho and Cr peaks were identified upon their ppm scale, volume and localisation (Figure 11). The obtained data was correlated with the animal reference values (Carrera, et al., 2014). NAA-to-choline ratio, NAA-to-creatine ratio, and choline-to-creatine and choline-to-NAA ratio were automatically calculated using resonance areas for both groups of dogs. Both groups were compared and the results were correlated with the available references from Warrington (Warrington et al., 2013).

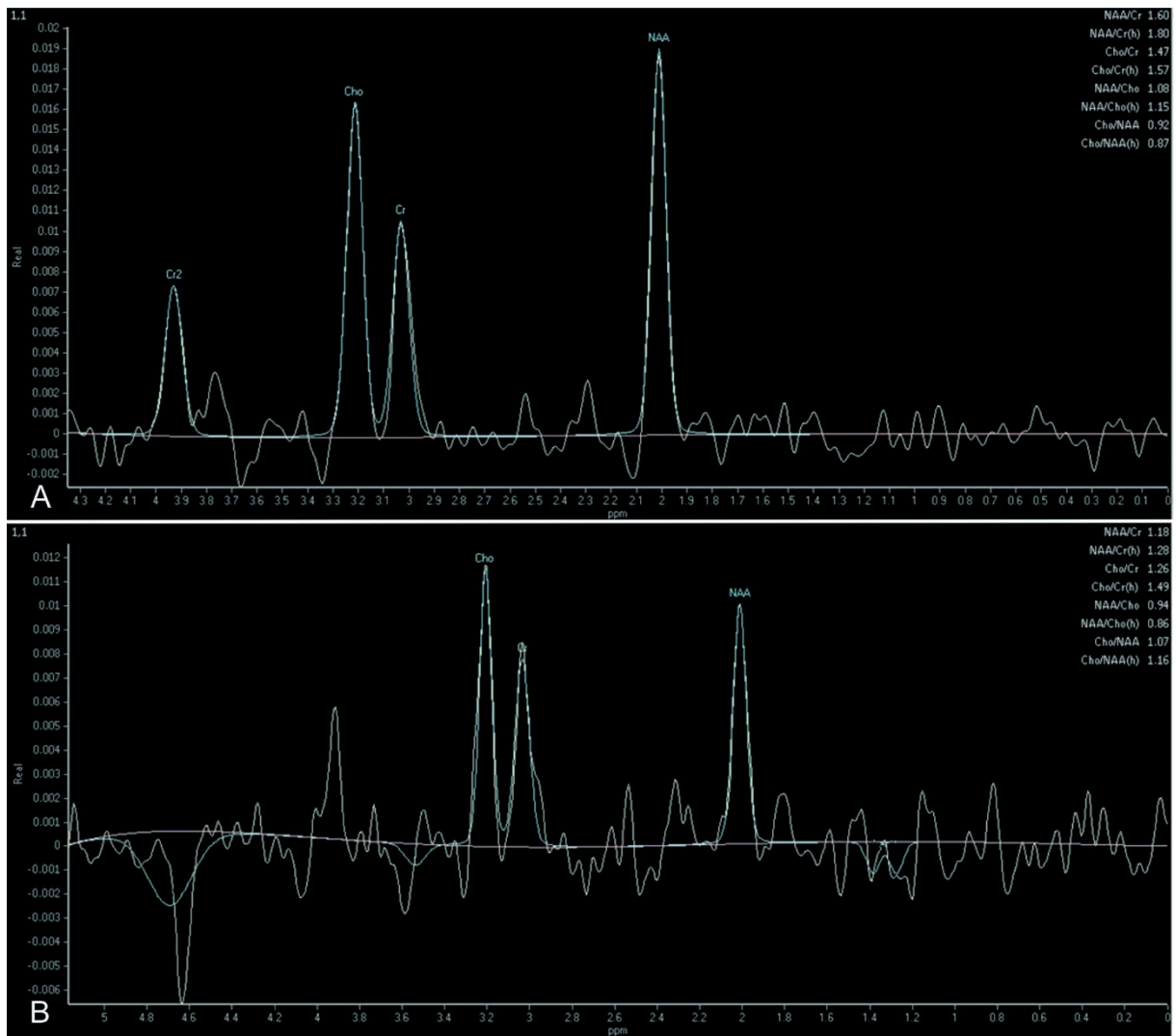


Figure 11: Single spectrum from an individual voxel placed at the level of temporal lobe including an posterior part of hippocampus showing metabolite peaks of NAA at 2.0 ppm, Cr at 3.0 ppm, Cho at 3.2 ppm and the calculated metabolite ratios in a mixed breed dog with degenerative disc disease included in the control group (A) and in 5 year old mixed breed male dog with idiopathic epilepsy and last seizure 5 days ago (B). The correlation between NAA, Cr and Cho metabolite peak varies between two dogs.

3.2.7 Statistical analysis

The collected data were analysed using statistical software (BMDP/ Dynamic, Statistical Software, Inc., Release 8.1). Descriptive statistics were calculated for peak area ratios at MR spectroscopy. The statistical evaluation included 4 metabolite ratios (NAA-to-choline ratio, NAA-to-creatine ratio, and choline-to-creatine and choline-to-NAA ratio) evaluated equally for both groups. The summary statistics over all cases and broken down by individual category on the group, was performed. The mean, standard deviation (SD), standard error of the mean (SE), the coefficient of variation (CV) the smallest value, the largest value and range were calculated for every category group including all dogs, age of dogs and all metabolite ratios (NAA-to-choline ratio, NAA-to-creatine ratio, choline-to-creatine and choline-to-NAA ratio) for the left and right side (amygdala and a posterior part of the hippocampus).

A two-factor repeated measures ANOVA test with respect to a side was used to compare the ratio values of the healthy dogs in the control group to the epileptic dogs in the study group. The cell mean, standard deviation and the analysis of variance was calculated for every dependent variable (DV) (NAA/Cr, Cho/Cr, NAA/Cho, Cho/NAA). An explorative data analysis was carried out to verify the relationship between the age (covariate) and gender (additional grouping) of canines and the metabolite ratio in different group variants.

A three-factor analysis of covariance (ANCOVA) with repeated measure with respect to a side was used to examine the correlation between the metabolite ratios and the age and sex of the diseased dogs. The same analysis was performed in the control group.

Single-factor analysis of covariance (ANCOVA) with repeated measures was applied to examine the correlation between the values of the metabolite ratios in dogs with epileptic seizures and time from the last seizure. The normal distribution was given for all variables, approximately. The level of significance (p) was considered significant < 0.05 for all applied tests.

4. Results

Twenty- seven dogs with idiopathic epilepsy met the inclusion criteria for our study. A list of dog breeds, their age and gender in the groups are summarised below (Table 1). All epileptic dogs (100%) showed no structural lesions in the MRI. Of ten dogs included in the control group, four were diagnosed with syringomyelia (40%), three with degenerative disc disease (30%), two with fibrocartilaginous embolism (20%) and one with spine trauma (10%). Table 2 presents the number of the dogs in the control group. Of twenty-seven canines in the study group, fifteen were male (56%) and twelve were female (44%), whereas in the control group three were male (30%) and seven female (70%). All dogs in the study group showed generalized tonic-clonic seizures with bilateral involvement, salivation and urination.

Seventeen dogs from the study group (63%) were categorised as with possible acute changes (≥ 14 days from the last seizure) while ten dogs (37%) with possible subacute changes (< 14 days the last seizure) (Figure 12).

The data for all variables (NAA/Cr, Cho/Cr, NAA/Cho, Cho/NAA) calculated for the control and diseased group were reviewed. All metabolite ratios calculated for the dogs in control and the study group are listed below (Table 3, 4).

Table 1: Number of different breed dogs comprised in the study group. Data included breed, sex, age in years and the time in days from the last seizure observed.

Breed	Sex	Age in years	Days from the last seizure
Bavarian Mountain dog	M	4	21
Central Asian Shepherd dog	F	2	27
Berger Blanc Suisse	M	2.5	2
Berger Blanc Suisse	M	2	20
Siberian Husky	F	3.5	28
Beagle	M	2	20
French bulldog	M	3	12
French bulldog	F	3	9
Bull terrier	M	5	1
Bull terrier	M	2	1
Mixed breed	M	5	7
Mixed breed	F	5	14
Dogo Argentino	M	1.5	15
Cocker spaniel	F	4	14
Border collie	F	1	21
Border collie	F	7	4
Miniature pinscher	F	1.6	7
Labrador retriever	F	3	0
Labrador retriever	M	1.5	1
Golden retriever	M	7	14
Hungarian Vizsla	F	3	15
American Staffordshire terrier	M	2	7
American Staffordshire terrier	M	7	0
Staffordshire Bull terrier	M	2	7
Mixed breed	F	7	14
Mixed breed	F	7	15
Rottweiler	M	2	28

Table 2: Dogs included in the control group. Data included breed predilection, sex, age and the diagnosis made based on the magnetic resonance examination.

Breed	Sex	Age in years	The reason for MRI
West Highland White terrier	M	3	Degenerative disc disease
Cavalier King Charles spaniel	F	2.4	Syringomyelia
Mixed dolichocephalic breed	M	4	Degenerative disc disease
Maltese	F	3.5	Syringomyelia
Labrador retriever	F	2	Fibrocartilaginous embolism
Cavalier King Charles spaniel	F	3	Syringomyelia
West Highland White terrier	F	1	Spinal trauma
Cavalier King Charles spaniel	F	2.5	Syringomyelia
French bulldog	F	3	Degenerative disc disease
Labrador retriever	M	2.5	Fibrocartilaginous embolism

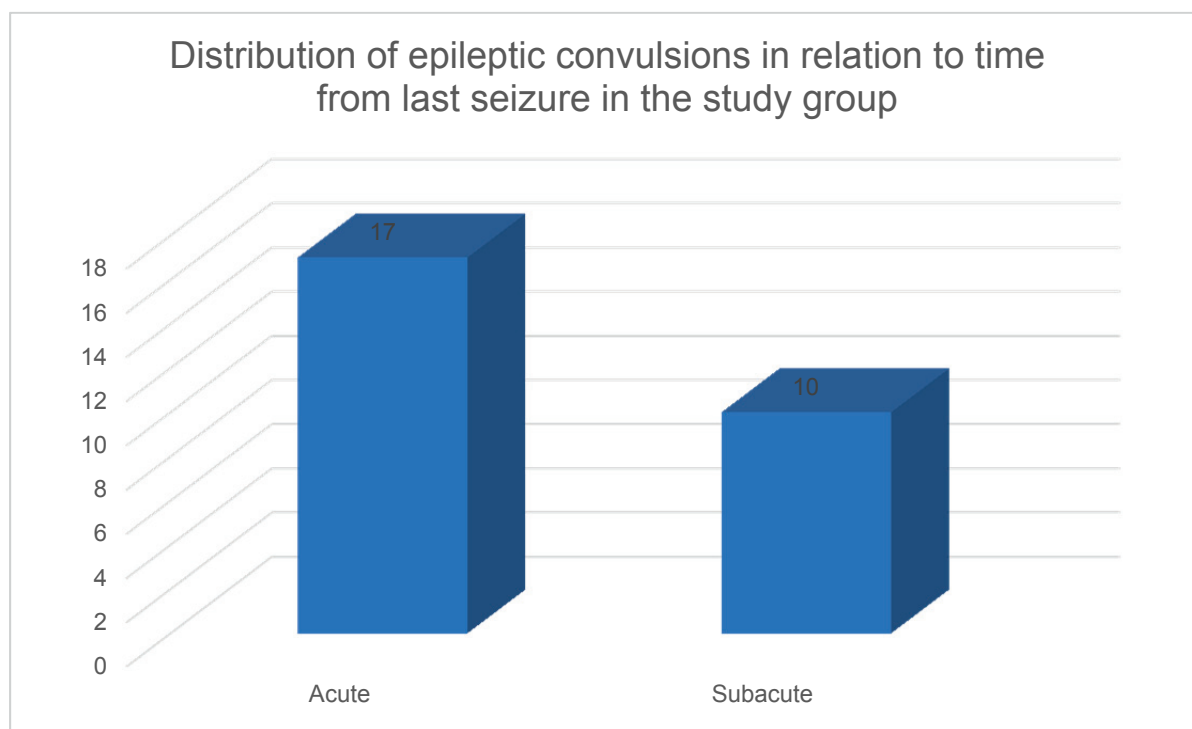


Figure 12: Graph showing a distribution of epileptic convulsions in relation to time from last seizure in dogs from the study group. Seventeen dogs were categorised as with possible acute changes while ten dogs with likely subacute changes.

Table 3: Calculated metabolite ratios (NAA/Cr, Cho/Cr, NAA/Cho, Cho/NAA) obtained at the level of the posterior part of the hippocampus and amygdala for the left and right side of 27 dogs with idiopathic epilepsy included in the study group.

Dog	Male / Female	Age (years)	LEFT SIDE				RIGHT SIDE			
			NAA / Cr	Cho / Cr	NAA / Cho	Cho / NAA	NAA / Cr	Cho / Cr	NAA / Cho	Cho / NAA
1	M	4	1.16	1.16	0.99	1.01	1.1	1.26	0.94	1.07
2	F	2	1.04	1.41	0.74	1.35	0.98	0.96	1.02	0.98
3	M	2.5	1.13	1.35	0.83	1.2	1.53	1.54	1	1
4	M	2	1.04	1.26	0.82	1.21	1.24	1.32	0.94	1.01
5	F	3.5	1.33	1.25	1.06	0.94	1.14	1.05	1.08	0.92
6	M	2	1.51	1.6	0.94	1.06	1.57	1.59	0.92	1.01
7	M	3	1.32	1.07	1.23	0.82	1.24	1	1.25	0.8
8	F	3	1.43	1.65	0.87	1.16	1.62	1.61	1	1
9	M	5	1.13	1.12	1.01	0.99	1.65	1.23	1.33	0.75
10	M	2	1.31	1.28	1.03	0.97	1.43	1.69	0.85	1.18
11	M	5	1.41	1.27	1.11	0.9	1.51	1.23	1.23	0.82
12	F	5	1.09	1.11	0.98	1.02	1.15	1.13	1.01	0.99
13	M	1.5	1.3	1.25	1.04	0.96	1.43	1.48	0.96	1.04
14	F	4	1.37	1.26	1.09	0.92	1.32	1.2	1.1	0.91

Dog	Male / Female	Age (years)	LEFT SIDE				RIGHT SIDE			
			NAA / Cr	Cho / Cr	NAA / Cho	Cho / NAA	NAA / Cr	Cho / Cr	NAA / Cho	Cho / NAA
15	F	1	1.64	1.02	1.61	0.62	1.43	1.13	1.27	0.79
16	F	7	1.31	1.1	1.19	0.84	1.31	1.14	1.15	0.87
17	F	1.6	1.18	1.19	0.99	1.01	1.07	1.12	0.96	1.05
18	F	3	1.51	1.1	1.38	0.73	1.76	1.27	1.39	0.72
19	M	1.5	1.04	0.92	1.13	0.89	1.6	0.8	2.02	0.5
20	M	7	1.25	1.24	1.01	0.99	1.66	1.13	1.47	0.68
21	F	3	1.49	1.25	1.2	0.84	1.48	1.1	1.35	0.74
22	M	2	1.44	1.33	1.08	0.92	0.99	0.94	1.05	0.95
23	M	7	1.37	1.18	1.17	0.86	1.48	1.75	0.85	1.18
24	M	2	1.51	1.06	1.43	0.7	1.53	1.29	1.18	0.85
25	F	7	1.06	1.21	0.87	1.15	1.3	1.44	0.9	1.11
26	F	7	1.63	1.37	1.19	0.84	1.93	1.55	1.24	0.8
27	M	2	1.38	1.91	0.72	1.39	1.33	2.01	0.66	1.51

Table 4: Calculated metabolite ratios (NAA/Cr, Cho/Cr, NAA/Cho, Cho/NAA) obtained at the level of the posterior part of the hippocampus and amygdala for the left and right side of 10 dogs included in the control group.

Dog	Age (years)	LEFT SIDE				RIGHT SIDE			
		NAA / Cr	Cho / Cr	NAA / Cho	Cho / NAA	NAA / Cr	Cho / Cr	NAA / Cho	Cho / NAA
1	3	0.88	0.92	0.96	1.04	1.43	1.23	1.16	0.86
2	2.4	1.51	1.31	1.15	0.87	1.67	1.47	1.13	0.88
3	4	1.27	1.47	0.87	1.15	1.03	1.24	0.83	1.2
4	3.5	1.34	1.1	1.22	0.82	1.32	1.05	1.26	0.8
5	2	1.57	1.43	1.1	0.91	1.41	1.06	1.34	0.75
6	3	1.83	1.29	1.42	0.7	1.9	1.21	1.57	0.64
7	1	1.7	1.1	1.54	0.65	1.41	1.19	1.19	0.84
8	2.5	1.32	1.37	0.97	1.03	1.65	1.32	1.25	0.8
9	3	1.25	1.17	1.07	0.94	1.43	1.25	1.15	0.87
10	2.5	1.36	1.4	0.97	1.03	1.52	1.36	1.12	0.9

Notable variations in the mean value of all variables (NAA/Cr, Cho/Cr, NAA/Cho, Cho/NAA) were observed among study and control group. NAA/Cr ratio had a mean value of 1.35 in the study group, whereas 1.44 in the control group. Cho/Cr ratio had a mean value of 1.28 in the study group, while 1.25 in the control group. NAA/Cho ratio had a mean value of 1.09 in the study group, whereas 1.16 in the control group. Cho/NAA ratio had a mean value of 0.95 in the study group, while 0.88 in the control group (Figure 13).

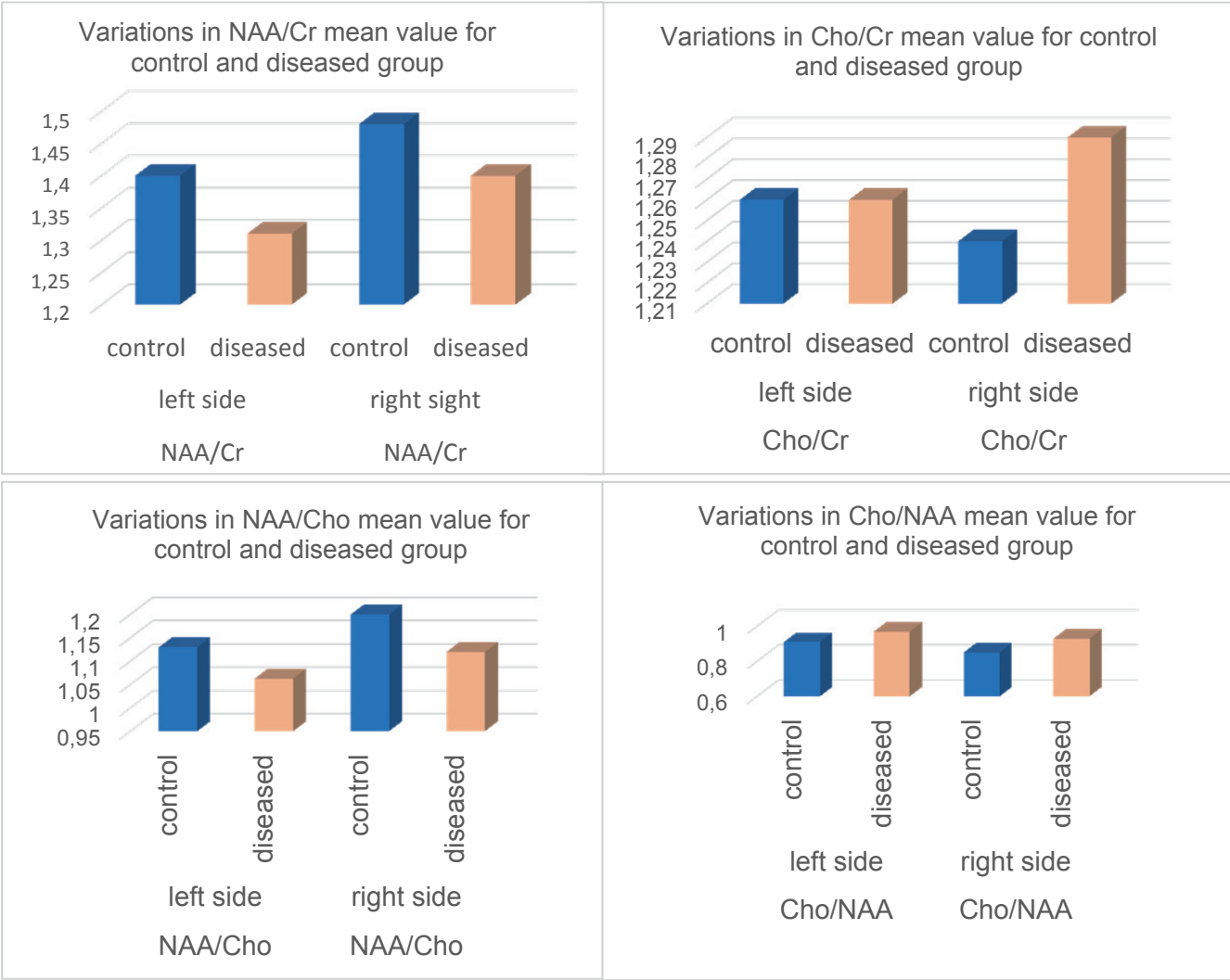


Figure 13: Graphs presenting the variations in metabolite mean values (NAA/Cr, Cho/Cr, NAA/Cho, Cho/NAA) between the control and epileptic dogs obtained in the region of left and right temporal lobe including a posterior part of hippocampus and amygdala.

A summary of metabolite ratios, mean and standard deviation, standard error of the mean, the coefficient of variation, the smallest value, the largest value in both groups is presented in Table 5.

4.1 Comparison of the metabolite ratios between the control and diseased group

No significant differences were observed, when comparing the metabolite ratios (NAA/Cr, Cho/Cr, NAA/Cho, Cho/NAA) between the control and diseased group. NAA/Cr had a level of significance (p) at 0.228, Cho/Cr at 0.228, NAA/Cho at 0.314 and Cho/NAA at 0.251 (Table 6). Moreover, the ratios for left and right region of interest similarly did not vary significantly between examined groups. Cho/Cr had a level of significance at 0.794, NAA/Cho at 0.149, Cho/NAA at 0.103. However, NAA/Cr value almost reached statistical difference ($p= 0.072$).

Table 5: Mean, standard deviations, standard error of mean, coefficient of variation, biggest and smallest values for calculated brain metabolite ratios of canines included in the control and diseased group.

Variable value	Side	Grouping	Total frequency	Mean	Standard deviation	Standard error of mean	Coefficient of variation	Smallest value	Largest
NAA/Cr	left	Control	10	1.40	0.27	0.084	0.19	0.88	1.83
		Disease	27	1.31	0.18	0.035	0.14	1.04	1.64
NAA/Cr	right	Control	10	1.48	0.23	0.073	0.16	1.03	1.90
		Disease	27	1.40	0.24	0.046	0.17	0.98	1.93
Cho/Cr	left	Control	10	1.26	0.18	0.056	0.14	0.92	1.47
		Disease	27	1.26	0.21	0.040	0.16	0.92	1.91
Cho/Cr	right	Control	10	1.24	0.13	0.040	0.10	1.05	1.47
		Disease	27	1.29	0.28	0.054	0.22	0.80	2.010
NAA/Cho	left	Control	10	1.13	0.21	0.068	0.19	0.87	1.54
		Disease	27	1.063	0.20	0.039	0.19	0.72	1.61
NAA/Cho	right	Control	10	1.20	0.19	0.059	0.16	0.83	1.57
		Disease	27	1.12	0.26	0.051	0.24	0.66	2.02
Cho/NAA	left	Control	10	0.91	0.16	0.050	0.17	0.65	1.15
		Disease	27	0.97	0.18	0.035	0.19	0.62	1.39
Cho/NAA	right	Control	10	0.85	0.14	0.045	0.17	0.64	1.20
		Disease	27	0.93	0.20	0.038	0.21	0.50	1.51

Table 6: Comparison of the metabolite ratios (NAA/Cr, Cho/Cr, NAA/Cho, Cho/NAA) between the control and diseased group. The examined ratios for left and right region of interest similarly showed no significant difference between groups.

Metabolite ratio	Main effects		
	Comparison between groups	Comparison between the sides	Interaction between the effect on the group and side
	<i>p</i> value	<i>p</i> value	<i>p</i> value
NAA/Cr	0.228	0.072	0.866
Cho/Cr	0.228	0.794	0.474
NAA/Cho	0.314	0.149	0.808
Cho/NAA	0.251	0.103	0.728

4.2 Correlation between the metabolite ratios and the age and sex

There was no significant decrease with advancing age for all examined metabolite ratios (NAA/Cr, $p= 0.598$; Cho/Cr, $p= 0.862$; NAA/Cho, $p= 0.898$; Cho/NAA, $p= 0.788$).

Similarly, no significant correlation between sex of the examined dogs was observed, when comparing the metabolite ratios in the control and diseased group (NAA/Cr, $p=0.0633$; Cho/Cr, $p= 0.517$; NAA/Cho, $p=0.065$; Cho/NAA, $p=0.063$).

Statistics data is presented in Table 7.

Table 7: A three- factor analysis of covariance (ANCOVA) with repeated measure with respect to a side used to examine the correlation between the metabolite ratios and the age and sex of the diseased dogs. No significant differences in metabolite ratios were found when comparing healthy and diseased group regarding age and sex.

Metabolite ratio	Main effects				Interactions				
	Group	Sex	Side		group x sex	group x side	sex x side	sex x group x side	Covariate age
	p value	p value	p value		p value	p value	p value	p value	p value
NAA/Cr	0.615	0.063	0.064		0.063	0.881	0.26	0.918	0.598
Cho/Cr	0.856	0.517	0.778		0.781	0.621	0.387	0.733	0.862
NAA/Cho	0.807	0.065	0.168		0.176	0.732	0.623	0.976	0.898
Cho/NAA	0.654	0.063	0.108		0.194	0.672	0.832	0.712	0.788

4.3 Correlation between the metabolite ratios and the time from the last seizure in the group of the diseased dogs

When interpreting the estimated regression coefficients, NAA/Cr and NAA/Cho ratios tend to decrease over time. In contrary, the values of Cho/Cr and Cho/NAA ratios increase with advancing time from the last seizure.

An interesting association was found between two metabolite ratios (NAA/Cho, Cho/NAA) and time from the last epileptic convulsion. NAA/Cho ratio decreased significantly with advancing time from last seizure ($p= 0.03$). Equally, Cho/NAA ratio was significantly lower ($p= 0.01$) in dogs with recent seizures and was increasing within time.

NAA/Cr and Cho/Cr ratios showed no significant difference over time from the last seizure (Table 8). However, NAA/Cr ratio in relation to a side showed a significant correlation at $p=0.054$.

Table 8: Significant positive correlation found between NAA/Cho ratio ($p= 0.03$) and Cho/NAA ratio ($p= 0.01$) and time from last seizure in comparison to the control group. Calculated regression coefficients show, how the metabolite ratio decreases (NAA/Cr, NAA/Cho) and increases (Cho/Cr, Cho/NAA) over time. Significant differences are highlighted in red.

Metabolite ratio	Main effects		Regression coefficients
	Last seizure	Side	
	<i>p</i> value	<i>p</i> value	
NAA/Cr	0.121	0.054	-0.005
Cho/Cr	0.169	0.364	0.006
NAA/Cho	0.026	0.275	-0.008
Cho/NAA	0.009	0.243	0.008

5. Discussion

In this study, we present data of interictal single-voxel MRSI of the temporal region in dogs with idiopathic epilepsy and structurally normal brain. No significant changes of investigated metabolite ratios were observed in the study cohort compared to controls. A relation between metabolite ratios and the time from the last seizure was found, i.e., the closer MRSI was obtained from the time of the last seizure, the higher was NAA/Cho ratio. NAA is one of the most abundant amino acids in the central nervous system. It is believed to be located primarily within neurons, where it is involved in energy metabolism (Miyake et al., 1981). It was also suggested to play a role in the synthesis of myelin and lipids in the central nervous system (Moffett et al., 2007). Loss of NAA signals is considered to be consistent with loss of neuronal integrity, but it can also be used as a marker of impaired neuronal function and reduced oxidative metabolism (Woermann et al., 1999). Concentrations of Cho and Cr are higher in astrocytes, which is why the change in the NAA/Cho and NAA/Cr ratios are considered to reflect neuronal loss and reactive astrocytosis as in humans with hippocampus sclerosis (Kendall et al., 2014; Stagg et al., 2013; Mellema et al., 1999).

In human patients with epilepsy, spectroscopic studies of the hippocampus are mainly used to determine lateralization of the epileptogenic zone in one temporal lobe. Unilateral decrease of NAA/Cr, NAA/Cho, or NAA/Cr ratios showed good concordance with localization of the epileptogenic zone in the respective hippocampus (Hetherington et al., 1995; Li et al., 2000) and predicts positive surgical outcome (Suhy et al., 2002). Furthermore, resection of the hippocampus is also performed in patients with structural or functional extra-temporal seizure foci if changes in the hippocampus can be detected (Condon et al., 2011; Li et al., 1997; Li et al., 1999). The presence of hippocampal damage and/or dysfunction, in association with a lesion outside the temporal lobe, is assumed to be due to propagation of epileptogenic activity from the remote focus into the hippocampus formation inducing secondary epileptogenic effects (Miller et al., 2000). Interictal spectroscopic examination revealed reduced hippocampal NAA/Cr and NAA/Cho in humans with extra-temporal epilepsy (Miller et al., 2000; Mueller et al., 2006). Surgical resection of the hippocampus can significantly reduce the seizure

frequency in these patients, which underlines the role of hippocampal propagation of seizure activity in presence of an extratemporal focus (Levesque et al., 1991).

Our understanding of epilepsy in dogs is still limited and somewhat focused on the existence of primary temporal lobe epilepsy (Hasegawa et al., 2016). However, the proof of any negative effect of the hippocampus on seizure generation or enhancement in epileptic dogs might take us a step forward and might encourage veterinary neurosurgeons to consider resection of the temporal lobe in dogs with refractory epilepsy (Estey et al., 2017). The finding of this study, namely that generalized tonic-clonic seizures do not create changes in metabolic spectra measured in the hippocampus, suggests that repeated seizures do not cause secondary damage to the hippocampus in dogs. However, the fact that other studies documented functional or structural changes of the hippocampus (Czerwik et al., 2018; Estey et al., 2017; Hartmann et al., 2017; Kuwabara et al., 2010) warrants further investigations using MRSI.

The role of the hippocampus and the presence of primary temporal lobe epilepsy in dogs is still a matter of debate. Although some evidence exists for some role of the temporal structures in the propagation and/or initiation of electrical activity (Montgomery et al., 1983; Yamasaki et al., 1991), no data has been published on the larger group of epileptic dogs. However, there is growing number of reports in veterinary medicine about temporal structures and their functional abnormalities including EEG abnormalities (Berendt et al., 1999; Czerwik et al., 2018; Hasegawa et al., 2003), MRI changes such as hyperintensity, hippocampal necrosis (Hasegawa, 2005), volume loss and ADC increase in diffusion weighted imaging (Hartmann et al., 2017; Kuwabara et al., 2010; Vullo et al., 1996).

In the histopathological examinations of the hippocampus typical findings include neuronal loss, most severely in the hilus of the dentate gyrus, axon reorganisation, hippocampal atrophy and sclerosis, temporal lobe sclerosis, cytotoxic oedema and gliosis. These variations and their functional consequences occur as a primary lesion that is the consequence of unknown insults, but can also arise as a secondary lesion after seizures originating elsewhere in the brain of humans and cats (Wagner et al., 2014). Macroscopically, hippocampal sclerosis can be characterized by an atrophic, small hippocampus that can be seen in MRI. Visual assessment of hippocampal atrophy that can be confirmed by postprocessing volumetric

techniques is usually the first feature indicating structural changes of the hippocampus (Wrzosek et al., 2016).

In humans, temporal lobe epilepsy with hippocampal sclerosis has a characteristic seizure semiology. A variety of autonomic and emotional symptoms can occur in the preictal phase, the complex partial seizure typically begins with motor arrest and staring followed by oroalimentary automatisms (e.g., lip-smacking, chewing) and other purposeless movements (Engel et al., 2006; Williamson et al., 1998). Secondary generalizations of seizures are frequently observed. Similar clinical findings were already documented in some dogs (Hasegawa et al., 2003; 2005) describing the temporal lobe to be the symptomatogenic region of seizure involvement. In the present report, all dogs included in the study group showed symptoms of jaw snapping, muscle rigidity, paddling of the legs, salivation, barking, jerking motions of the muscles, stiffening of the legs and neck, which can occur in primary temporal lobe epilepsy. Aggression, fear and other behavioural changes followed by secondary generalization of seizures were also mentioned which could suggest the involvement of temporal structures (Hasegawa et al., 2005; Mellema et al., 1999). The primary origin of the hippocampus in the seizure events therefore cannot be excluded.

5.1 Limitations of the study

The results of our study might have been biased due to a number of reasons. Although we could not document a correlation between the duration of seizure activity before imaging, influence of seizure frequency and duration cannot be ruled out. Humans with TLE studied within 24 hours postictal period showed no changes in the metabolite ratios suggesting that this ratio is insensitive to immediate seizure history (Cendes et al., 1997; Maton et al., 2001). Another study found no relationship between NAA/Cho, NAA/Cr and seizure duration, frequency, or lifetime estimated seizures (Warrington et al., 2013). We found a correlation between time duration to the last seizure and decrease of NAA/Cho. If all dogs would have been examined at comparable time duration to the last seizure, the differences in the metabolite ratios might have become significant. The difference between ratios between left and right

hippocampal formation almost reached significance, which might also increase with standardized imaging modalities. These possible connections should be further investigated.

We decided for single voxel measurement as it provides volume selectivity of the acquired signal and therefore high signal-to-noise ratio resulting in high-quality spectra suitable for quantitative analysis. However, using single-voxel acquisition, it was technically not possible to reduce the voxel < 1 cm in size. Therefore, the spectra were not measured exclusively in the temporal lobe, but contained information from adjacent brain tissue, especially from the thalamus. This was technically unavoidable because of the placement of the voxel outside of the margins of the brain, thus overlapping the calvaria and producing poor-quality spectra due to fat contamination (Ober et al., 2013). However, this can be seen as a systematic error that occurred in every examined dog.

Multivoxel acquisition techniques offer the advantage of examining smaller regions of interest, which is important when studying small or irregularly shaped anatomic structures as the hippocampus formation. However, spectral contamination from adjacent voxels can have a high influence on the values, which makes quantification of the spectra difficult. Ratios determined by Warrington, obtained in the temporal lobe of 10 healthy beagles were higher than in our control group (Warrington et al., 2013). Both absolute values and NAA/Cho, NAA/Cr and Cho/Cr ratios have a larger range and median values, which probably reflect the differences of single- vs multivoxel acquisition. Systematic comparison between spectroscopic data obtained by single- and multi-voxel acquisition has been performed in dog cadavers (Ober et al., 2013). According to the recent preliminary findings (Lee et al., 2018), single- and multi-voxel spectroscopy techniques yield comparable results for similar sized regions of interest in the normal canine brain.

The absolute metabolite quantification can be obtained in two different ways: as ratios or absolute metabolite concentrations. The results of our spectra are expressed in terms of ratios which are considered to be a more stable indicator to describe parenchymal changes (Li et al., 2003; Kuzniecky et al., 2015). The major disadvantage of the quantification as absolute metabolite concentrations is that several advanced spectral fitting techniques measured by dedicated software must be carried on in order to obtain relevant measurements.

We decided to use the long echo time PRESS sequence because of the improved signal intensity-to-noise ratio and a more readable spectrum which contains less signal from the lipid and metabolites with short T2 values, thus helps to interpret the spectrum. In contrary, STEAM technique is obtained using shorter echo times which enables detection of small metabolites with shorter T2 times (Castillo et al., 1996; Kwock et al., 1998). Further studies examining PRESS and STEAM techniques simultaneously need to be performed.

It is also unclear as to whether the measured spectra and ratios might be breed specific, or breed specifically biased. We included brachycephalic dogs to our control group. The brains of these dogs are somewhat distorted, which might have caused slightly different tissue components in the examined voxels. Hippocampal volume differs significantly in size in allometric relationships to brain- and bodyweight. Comparisons between larger cohorts of homogenous groups of dogs of the same breed will be necessary to prove such a breed influence on MRSI spectra. In humans, metabolite ratios can differ along the long axis of the hippocampus with lower ratios of NAA/Cho and NAA/Cr in the anterior as compared with the posterior part of the hippocampus (Vermathen et al., 2000). We examined only a posterior part of the hippocampus, therefore further studies are needed to compare it to the other area.

Last, the MRI of the control group was performed after examination of other body parts, which likely increase time under general anaesthesia and therefore could possibly alter brain metabolism.

The variability of the technical parameters used for spectroscopic investigations and the absence of standard criteria for dogs both for spectral acquisition and data analysis make the interpretation of results of magnetic resonance spectroscopy in veterinary patients challenging.

6. Conclusion

Interictal single voxel proton magnetic resonance spectroscopy ($^1\text{HMRS}$) of the temporal region in dogs with idiopathic epilepsy and structurally normal MRI revealed no statistically relevant changes in examined metabolite ratios (NAA/Cr, Cho/Cr, NAA/Cho, Cho/NAA) in comparison to the healthy group. NAA/Cho ratios negatively correlate with time duration to seizure.

7. Summary

Single voxel proton magnetic resonance spectroscopy is a promising diagnostic tool for use in dogs with idiopathic epilepsy und structurally normal brain. We did not observe variations in the investigated metabolite ratios in the IE group compared to the controls. Moreover, no age and sex related differences in metabolite ratios were noted. However, there is strong evidence for a relation between metabolite ratios and the time from the last seizure. Our data strongly suggests, that further MRS studies should be obtained on dogs in the ictal period. Magnetic resonance spectroscopy presents an additional value for the diagnosis of the canine idiopathic epilepsy and could help to localize the epileptogenic region in the future.

8. Zusammenfassung

Die Single- Voxel- Protonen- Magnetresonanz- Spektroskopie ist ein erfolgversprechendes Diagnosewerkzeug für Hunde mit idiopathischer Epilepsie und strukturell normalem Gehirn. In den untersuchten Metabolitenverhältnissen- in der Gruppe mit idiopathischer Epilepsie- haben wir im Vergleich zur Kontrollgruppe keine Unterschiede beobachtet. Darüber hinaus wurden keine alters- und geschlechtsspezifischen Unterschiede in den Metabolitenverhältnissen festgestellt. Es gibt jedoch deutliche Belege für einen Zusammenhang zwischen Metabolitenverhältnissen und der Zeit seit dem letzten epileptischen Anfall. Unsere Daten deuten stark darauf hin, dass weitere MRS-Studien an Hunden in der iktalen Phase durchgeführt werden sollten. Die Magnetresonanzspektroskopie stellt einen

zusätzlichen Wert für die Diagnose der idiopathischen Epilepsie beim Hund dar und könnte dazu beitragen, die epileptogene Areal in Zukunft zu lokalisieren.

9. Acknowledgments

Most of all, I would like to acknowledge Prof. Dr. med. vet. Martin J. Schmidt and Dr. hab. Marcin Wrzosek who have challenged and enriched my ideas during the doctoral studies. I would also like to thank my family for their continuous love, support, and constant encouragement I have received over the years.

8. References

- Amaral, D. G., Witter, M. P. (1989). The three-dimensional organization of the hippocampal formation: A review of anatomical data. *Neuroscience*; 31, 571-591.
- Ackerstaff, E., Glunde, K., Bhujwala, Z. M. (2003). Choline phospholipid metabolism: A target in cancer cells? *Journal of Cellular Biochemistry*, 90(3), 525-533.
- Alger, J. R. (2010). Quantitative proton magnetic resonance spectroscopy and spectroscopic imaging of the brain: a didactic review. *Topics in Magnetic Resonance Imaging : TMRI*, 21(2), 115-128.
- Ang, C. W., Carlson, G. C., Coulter, D. A. (2008). Massive and Specific Dysregulation of Direct Cortical Input to the Hippocampus in Temporal Lobe Epilepsy. *The Journal of Neuroscience*, 26(46), 1850-1856.
- Arnold, D. L., Matthews, P. M., Francis, G. S., O'Connor, J., Antel, J. P. (1992). Proton magnetic resonance spectroscopic imaging for metabolic characterization of demyelinating plaques. *Annals of Neurology*, 31(3), 235-241.
- Azab, S. F., Sherief, L. M., Saleh, S. H., Elshafeiy, M. M., Siam, A. G., Elsaeed, W. F., Aziz, K.A. (2015). Childhood temporal lobe epilepsy: correlation between electroencephalography and magnetic resonance spectroscopy: a case-control study. *Italian Journal of Pediatrics*, 41(1), 32.
- Aziz, A., Aun, K., Ahmed, A., Mohamed, A., Fotouh, A., Saeed, K., Muayad, O. (2016). Role of magnetic resonance spectroscopy (MRS) in nonlesional temporal lobe epilepsy. *The Egyptian Journal of Radiology and Nuclear Medicine*, 47(1), 217-231.
- Barker, P. B., Bizzi, A., DeStefano, N., Gullapalli, R., Lin, D. D. M. (2011). *Clinical MR Spectroscopy Techniques and Applications* (Vol. 1). Cambridge University Press, New York.

- Barker, P. B., Breiter, S. N., Soher, B. J., Chatham, J. C., Forder, J. R., Samphilipo, M. A., Anderson, J. H. (1994). Quantitative proton spectroscopy of canine brain: in vivo and in vitro correlations. *Magnetic Resonance in Medicine*, 32(2), 157-163.
- Battini, R., Leuzzi, V., Carducci, C., Tosetti, M., Bianchi, M. C., Item, C. B., Cioni, G. (2002). Creatine depletion in a new case with AGAT deficiency: clinical and genetic study in a large pedigree. *Molecular Genetics and Metabolism*, 77(4), 326-331.
- Beckmann, K., Carrera, I., Steffen, F., Golini, L., Kircher, P. R., Schneider, U., Bley, C. (2015). A newly designed radiation therapy protocol in combination with prednisolone as treatment for meningoencephalitis of unknown origin in dogs: a prospective pilot study introducing magnetic resonance spectroscopy as monitor tool. *Acta Veterinaria Scandinavica*, 57(1), 4.
- Behar, K. L., den Hollander, J., Stromski, M. E., Ogino, T., Shulman, R. G., Petroff, O., Prichard, J. W. (1983). High-resolution ¹H nuclear magnetic resonance study of cerebral hypoxia in vivo. *Proceedings of the National Academy of Sciences of the United States of America*, 80(16), 4945-4948.
- Behr, J., Lyson, K. J., Mody, I. (1998). Enhanced Propagation of Epileptiform Activity Through the Kindled Dentate Gyrus. *Journal of Neurophysiology*, 79(4), 1726-1732.
- Ben-Ari, Y., Tremblay, E., Ottersen, O. P., Meldrum, B. S. (1980). The role of epileptic activity in hippocampal and "remote" cerebral lesions induced by kainic acid. *Brain Research*, 191(1), 79-97.
- Berendt, M., Høgenhaven, H., Flagstad, A., Dam, M. (1999). Electroencephalography in dogs with epilepsy: similarities between human and canine findings. *Acta Neurologica Scandinavica*, 99(5), 276-283.
- Bernasconi, A., Bernasconi, N., Natsume, J., Antel, S. B., Andermann, F., Arnold, D. L. (2003). Magnetic resonance spectroscopy and imaging of the thalamus in idiopathic generalized epilepsy. *Brain*, 126(11), 2447-2454.

- Bernasconi, A., Tasch, E., Cendes, F., Li, L. M., Arnold, D. L. (2002). Proton magnetic resonance spectroscopic imaging suggests progressive neuronal damage in human temporal lobe epilepsy. *Progress in Brain Research*, 135, 297-304.
- Bertram, E. (2007). The relevance of kindling for human epilepsy. *Epilepsia*, 48(2), 65-74.
- Bitsch, A., Bruhn, H., Vougioukas, V., Stringaris, A., Lassmann, H., Frahm, J., Brück, W. (1999). Inflammatory CNS demyelination: Histopathologic correlation with in vivo quantitative proton MR spectroscopy. *American Journal of Neuroradiology*, 20(9), 1619-1627.
- Blümcke, I. (2009). Epilepsy & Behavior Neuropathology of focal epilepsies: A critical review. *Epilepsy and Behavior*, 15(1), 34-39.
- Blümcke, I., Thom, M., Wiestler, O. D. (2002). Ammon's horn sclerosis: a maldevelopmental disorder associated with temporal lobe epilepsy. *Brain Pathology*, 12(2), 199-211.
- Bouchet, C., Cazauvieilh, C., A. (1825). De l'épilepsie considérée dans ses rapports avec l'aliénation mentale. Recherche sur la nature et le siège de ces deux maladies. *Archives of General Internal Medicine*, 510-542.
- Braissant, O. (2010). Ammonia toxicity to the brain: Effects on creatine metabolism and transport and protective roles of creatine. *Molecular Genetics and Metabolism*, 100 (1), S53-S58.
- Braissant, O., Henry, H., Loup, M., Eilers, B., Bachmann, C. (2001). Endogenous synthesis and transport of creatine in the rat brain: An in situ hybridization study. *Molecular Brain Research*, 86(1-2), 193-201.
- Braissant, O., Henry, H., Villard, A. M., Zurich, M. G., Loup, M., Eilers, B., Bachmann, C. (2002). Ammonium-induced impairment of axonal growth is prevented through glial creatine. *The Journal of Neuroscience*, 22(22), 9810-9820.

- Buckmaster, P. S., Smith, M. O., Buckmaster, C. L., Lecouteur, R. A., Dudek, F. E. (2002). Absence of Temporal Lobe Epilepsy Pathology in Dogs with Medically Intractable Epilepsy, *Journal of Veterinary Internal Medicine*, 16(1): 95-99.
- Burri, R., Steffen, C., Herschkowitz, N. (1991). N-acetyl-L-aspartate is a major source of acetyl groups for lipid synthesis during rat brain development. *Developmental Neuroscience*, 13(6), 403-411.
- Calcagnotto, M. E., Barbarosie, M., Avoli, M. (2000). Hippocampus-entorhinal cortex loop and seizure generation in the young rodent limbic system. *Journal of Neurophysiology*, 83, 3183-3187.
- Carrera, I., Kircher, P. R., Meier, D., Richter, H., Beckman, K., Dennler, M. (2014). In vivo proton magnetic resonance spectroscopy for the evaluation of hepatic encephalopathy in dogs. *American Journal of Veterinary Research*, 75(9), 818-827.
- Carrera, I., Richter, H., Meier, D., Kircher, P. R., Dennler, M. (2015). Regional metabolite concentrations in the brain of healthy dogs measured by use of short echo time, single voxel proton magnetic resonance spectroscopy at 3.0 Tesla. *American Journal of Veterinary Research*, 76(2), 129-141.
- Cascino, G. D., Jack, C. R., Parisi, J. E. (1993). Operative strategy in patients with MRI-identified dual pathology and temporal lobe epilepsy. *Epilepsy Research* 14, 175-82.
- Castillo, M., Kwock, L., Mukherji, S. K. (1996). Clinical applications of proton MR spectroscopy. *American Journal of Neuroradiology*, 17, 1–15.
- Cendes, F., Andermann, F., Dubeau, F., Matthews, P. M., Arnold, D. L. (1997). Normalization of neuronal metabolic dysfunction after surgery for temporal lobe epilepsy. Evidence from proton MR spectroscopic imaging. *Neurology*, 49(6), 1525-1533.
- Cendes, F., Andermann, F., Gloor, P., Evans, A., Jones-Gotman, M., Watson, C., Lopes-Cendes, I. (1993). MRI volumetric measurement of amygdala and hippocampus in temporal lobe epilepsy. *Neurology*, 43(4), 719-725.

- Cendes, F., Andermann, F., Preul, M. C., Arnold, D. L. (1994). Lateralization of temporal lobe epilepsy based on regional metabolic abnormalities in proton magnetic resonance spectroscopic images. *Annals of Neurology*, 35(2), 211-216.
- Chan, S., Chin, S. S. M., Kartha, K., Nordli, D. R., Goodman, R. R., Pedley, T., Hilal, S. K. (1996). Reversible Signal Abnormalities in the Hippocampus and Neocortex after Prolonged Seizures. *American Journal of Neuroradiology*, 1725-1731.
- Chapman, A. G. (1998). Glutamate receptors in epilepsy. *Progress in Brain Research*, 116, 371-383.
- Chatham, J. C., Blackband, S. J. (2001). Nuclear magnetic resonance spectroscopy and imaging in animal research. *ILAR Journal / National Research Council, Institute of Laboratory Animal Resources*, 42(3), 189-208.
- Chen, J. W. Y., Naylor, D. E., & Wasterlain, C. G. (2007). Advances in the pathophysiology of status epilepticus. *Acta Neurologica Scandinavica*. 186, 7-15.
- Chiu, P. W., Mak, H. K. F., Yau, K. W., Chan, Q., Chang, R. C., Chu, L. W. (2014). Metabolic changes in the anterior and posterior cingulate cortices of the normal aging brain: proton magnetic resonance spectroscopy study at 3 T. *Age*, 36(1), 251-264.
- Condon, B. (2011). Magnetic resonance imaging and spectroscopy: How useful is it for prediction and prognosis? *EPMA Journal*, 2(4), 403-410.
- Connelly, A., Jackson, G. D., Duncan, J. S., King, M. D., Gadian, D. G. (1994). Magnetic resonance spectroscopy in temporal lobe epilepsy. *Neurology*, 44(8), 1411-1417.
- Connett, R. J. (1988). Analysis of metabolic control: new insights using scaled creatine kinase model. *The American Journal of Physiology*, 254(6), 949-959.

- Cook, M. J., Fish, D. R., Shorvon, S. D., Straughan, K., Stevens, J. M. (1992). Hippocampal volumetric and morphometric studies in frontal and temporal lobe epilepsy. *Brain : A Journal of Neurology*, 115(4), 1001-1015.
- Dewey C. W., da Costa, R.C. (2016). *Practical Guide to Canine and Feline neurology* (Third Edition). Wiley Blackwell.
- Czerwik A., Płonek M., Podgórski P., Wrzosek M. (2018). Comparison of electroencephalographic findings with hippocampal magnetic resonance imaging volumetry in dogs with idiopathic epilepsy. *Journal of Veterinary Internal Medicine* 1-8.
- De Deyn, P. P., Marescau, B., MacDonald, R. L. (1990). Epilepsy and the GABA-hypothesis a brief review and some examples. *Acta Neurologica Belgica*, 90(2), 65-81.
- De Stefano, N., Narayanan, S., Francis, S. J., Smith, S., Mortilla, M., Tartaglia, M. C., Arnold, D. L. (2002). Diffuse axonal and tissue injury in patients with multiple sclerosis with low cerebral lesion load and no disability. *Archives of Neurology*, 59(10), 1565-71.
- DeLahunta, A., Glass, E. (2015). *Veterinary Neuroanatomy and Clinical Neurology* (Fourth Edition). Saunders Elsevier, St. Louis.
- Desagher, S., Martinou, J. C. (2000). Mitochondria as the central control point of apoptosis. *Trends in Cell Biology*, 10(9), 369-377.
- Engel, J. J. (2006). ILAE classification of epilepsy syndromes. *Epilepsy Research*, 1, S5-10.
- Estey, C. M., Dewey, C. W., Rishniw, M. (2017). A subset of dogs with presumptive idiopathic epilepsy show hippocampal asymmetry: A volumetric comparison with non-epileptic dogs using MRI. *Frontiers in Veterinary Science*, 4, 183.
- Farber, J. L., Chien, K. R., Mittnacht, S. (1981). Myocardial ischemia: the pathogenesis of irreversible cell injury in ischemia. *The American Journal of Pathology*, 102(2), 271-281.

- Filibian, M., Frasca, A., Maggioni, D., Micotti, E., Vezzani, A., Ravizza, T. (2012). In vivo imaging of glia activation using ¹H-magnetic resonance spectroscopy to detect putative biomarkers of tissue epileptogenicity. *Epilepsia*, 53(11), 1907-1916.
- Fountain, N. B., Lothman, E.W. (1995). Pathophysiology of status epilepticus. *Journal of Clinical Neurophysiology*, 12(4), 326-342.
- Garcia, P. A., Laxer, K. D., van der Grond, J., Hugg, J. W., Matson, G. B., Weiner, M. W. (1995). Proton magnetic resonance spectroscopic imaging in patients with frontal lobe epilepsy. *Annals of Neurology*, 37(2), 279-281.
- Gideon, P., Sperling, B., Arlien-Soborg, P., Olsen, T. S., Henriksen, O. (1994). Long-term follow-up of cerebral infarction patients with proton magnetic resonance spectroscopy. *Stroke*, 25(5), 967-973.
- Green, D. R., Reed, J. C. (1998). Mitochondria and apoptosis. *Science*, 281(8), 1309-1312.
- Guevara, C. A., Blain, C. R., Stahl, D., Lythgoe, D. J., Leigh, P. N., Barker, G. J. (2010). Quantitative magnetic resonance spectroscopic imaging in Parkinson's disease, progressive supranuclear palsy and multiple system atrophy. *European Journal of Neurology*, 17(9), 1193-1202.
- Hagenfeldt, L., Bollgren, I., Venizelos, N. (1987). N-acetylaspartic aciduria due to aspartoacylase deficiency- a new aetiology of childhood leukodystrophy. *Journal of Inherited Metabolic Disease*, 10(2), 135-141.
- Hammen, T., Kuzniecky, R. (2012). *Magnetic resonance spectroscopy in epilepsy. Handbook of Clinical Neurology* (First Edition, Vol. 107). Elsevier, Burlington, USA.
- Harris, K., Lin, A., Bhattacharya, P., Tran, T., Wong, W., Ross, B. (2006). Regulation of NAA-Synthesis in the Human Brain in Vivo: Canavan's Disease, Alzheimer's Disease and Schizophrenia. In Moffett, J. R., Tieman, S. B., Weinberger, D. R., Coyle, J. T., Namboodiri, A. M. A. *N-Acetylaspartate: A Unique Neuronal Molecule in the Central Nervous System* (263–273). Boston, MA: Springer US.

- Hartmann, A., Sager, S., Failing, K., Sparenberg, M., Schmidt, M. J. (2017). Diffusion-weighted imaging of the brains of dogs with idiopathic epilepsy. *BMC Veterinary Research*, 13(1), 338.
- Hasegawa, D. (2016). Diagnostic techniques to detect the epileptogenic zone: Pathophysiological and presurgical analysis of epilepsy in dogs and cats. *The Veterinary Journal*. 215, 64-75.
- Hasegawa, D., Nakamura, S., Fujita, M., Takahashi, K., Orima, H. (2005). A dog showing Klüver-Bucy syndrome-like behavior and bilateral limbic necrosis after status epilepticus. *Veterinary Neurology & Neurosurgery Journal*, 7(1), 1.
- Hasegawa, D., Orima, H., Fujita, M., Nakamura, S., Takahashi, K., Ohkubo, S., Hashizume, K. (2003). Diffusion-weighted imaging in kainic acid-induced complex partial status epilepticus in dogs. *Brain Research*, 983(1-2), 115-127.
- Hauser, W. A., Annegers, J. F., Kurland, L. T. (1991). Prevalence of epilepsy in Rochester, Minnesota: 1940-1980. *Epilepsia*, 32(4), 429-445.
- Heinemann, U., Beck, H., Dreier, J. P., Ficker, E., Stabel, J., Zhang, C. L. (1992). The dentate gyrus as a regulated gate for the propagation of epileptiform activity. *Epilepsy Research*, 7, 273-280.
- Hetherington, H. P., Kuzniecky, R. I., Vives, K., Devinsky, O., Pacia, S., Luciano, D., Pan, J. W. (2007). A subcortical network of dysfunction in TLE measured by magnetic resonance spectroscopy. *Neurology*, 69(24), 2256-2265.
- Hetherington, H. P., Pan, J. W., Mason, G. F., Adams, D., Vaughn, M. J., Twieg, D. B., Pohost, G. M. (1996). Quantitative ¹H spectroscopic imaging of human brain at 4.1 T using image segmentation. *Magnetic Resonance in Medicine*, 36(1), 21-29.
- Hiremath, G. K., Najm, I. M. (2007). Magnetic resonance spectroscopy in animal models of epilepsy. *Epilepsia*, 48 (4), 47-55.

- Sievert, C. H., Richter, H. E., Beckmann, .A., Kircher, P, Carrera, I. (2016). Comparison between proton magnetic resonance spectroscopy findings in dogs with tick-borne encephalitis and clinically normal dogs. *Veterinary Radiology and Ultrasound*, 58(1), 53-61.
- Jack, C. R. J., Sharbrough, F. W., Cascino, G. D., Hirschorn, K. A., O'Brien, P. C., Marsh, W. R. (1992). Magnetic resonance image-based hippocampal volumetry: correlation with outcome after temporal lobectomy. *Annals of Neurology*, 31(2), 138-146.
- Jung, M. A., Nahm, S. S., Lee, M. S., Lee, I. H., Lee, A. R., Jang, D. P., Eom, K. D. (2010). Canine hippocampal formation composited into three-dimensional structure using MPRAGE. *The Journal of Veterinary Medical Science / the Japanese Society of Veterinary Science*, 72(7), 853-60.
- Kalachikov, S., Evgrafov, O., Ross, B., Winawer, M., Barker-Cummings, C., Martinelli Boneschi, F., Gilliam, T. C. (2002). Mutations in LGI1 cause autosomal-dominant partial epilepsy with auditory features. *Nature Genetics*, 30(3), 335-341.
- Kantarci, K., Shin, C., Britton, J. W., So, E. L., Cascino, G. D., Jack, C. R. J. (2002). Comparative diagnostic utility of 1H MRS and DWI in evaluation of temporal lobe epilepsy. *Neurology*, 58(12), 1745-1753.
- Kearsley-Fleet, L., O'Neill, D. G., Volk, H. A., Church, D. B., Brodbelt, D. C. (2013). Prevalence and risk factors for canine epilepsy of unknown origin in the UK. *Veterinary Record*, 172(13), 338-338.
- Kendall, G. S., Melbourne, A., Johnson, S., Price, D., Bainbridge, A., Gunny, R., Robertson, N.J. (2014). Ratios at MR Spectroscopy Are Predictive of Motor Outcome in Preterm Infants. *Radiology*, 271(1), 230-238.
- Khwaja, O., Volpe, J. J. (2008). Pathogenesis of cerebral white matter injury of prematurity. *Archives of Disease in Childhood. Fetal and Neonatal Edition*, 93(2), 153-161.

- Kleefstra, T., Rosenberg, E. H., Salomons, G.S., Stroink, H., van Bokhoven, H., Hamel, B. C. J., de Vries, B. B. A. (2005). Progressive intestinal, neurological and psychiatric problems in two adult males with cerebral creatine deficiency caused by an SLC6 A8 mutation. *Clinical Genetics*, 68(4), 379-381.
- Koestner, A. (1989). Neuropathology of canine epilepsy. *Problems in Veterinary Medicine*, 1(4), 516-534.
- Kuwabara, T., Hasegawa, D., Kobayashi, M., Fujita, M., Orima, H. (2010). Clinical magnetic resonance volumetry of the hippocampus in 58 epileptic dogs. *Veterinary Radiology and Ultrasound*, 51(5), 485-490.
- Kuzniecky, R., Hetherington, H., Pan, J., Hugg, J., Palmer, C., Gilliam, F., Morawetz, R. (1997). Proton spectroscopic imaging at 4.1 tesla in patients with malformations of cortical development and epilepsy. *Neurology*, 48(4), 1018-1024.
- Kuzniecky, R. I., Jackson, G. D. (2015). *Magnetic resonance in epilepsy: neuroimaging techniques*. Elsevier Academic, Burlington, USA.
- Kwock, L. (1998). Localized MR spectroscopy: basic principles. *Neuroimaging Clinics of North America*, 8, 713-31.
- Lane, S. B., Bunch, S. E. (1990). Medical management of recurrent seizures in dogs and cats. *Journal of Veterinary Internal Medicine*, 4(1), 26-39.
- Lanerolle, N. C. De, Kim, J., Spencer, D. D. (1989). Hippocampal interneuron loss and plasticity in human temporal lobe epilepsy. *Brain Research*, 495, 387-395.
- Lauriero, F., Federico, F., Rubini, G., Conte, C., Simone, I., Inchingolo, V., d'Addabbo, A. (1996). ⁹⁹Tcm-HMPAO SPET and ¹H-MRS (proton magnetic resonance spectroscopy) in patients with ischaemic cerebral infarction. *Nuclear Medicine Communications*, 17(2), 140-146.

- Lee, A. J., Beasley, M. D., Barrett, E. R., James, J., Gambino, J. (2018). Single-voxel and multi-voxel spectroscopy yield comparable results in the normal juvenile canine brain when using 3 Tesla magnetic resonance imaging. *Veterinary Radiology and Ultrasound*, 59(5), 577-586.
- Lei, H., Berthet, C., Hirt, L., Gruetter, R. (2009). Evolution of the Neurochemical Profile after Transient Focal Cerebral Ischemia in the Mouse Brain. *Journal of Cerebral Blood Flow & Metabolism*, 29(4), 811-819.
- Levesque, M. F., Nakasato, N., Vinters, H. V., Babb, T. L. (1991). Surgical treatment of limbic epilepsy associated with extrahippocampal lesions: the problem of dual pathology. *Journal of Neurosurgery*, 75, 364-370.
- Li, L. M., Andermann, F. (1999). Surgical outcome in patients with epilepsy and dual pathology. *Brain*, 122, 799-805.
- Li, L. M., Cendes, F., Antel, S. B. (2000). Prognostic value of proton magnetic resonance spectroscopic imaging for surgical outcome in patients with intractable temporal lobe epilepsy and bilateral hippocampal atrophy. *Annals of Neurology*, 47, 195-200.
- Li, L. M., Cendes, F., Watson, C., Andermann, F. (1997). Surgical treatment of patients with single and dual pathology: relevance of lesion and of hippocampal atrophy to seizure outcome. *Neurology*, 48, 437-44.
- Loffelholz, K., Klein, J., Koppen, A. (1993). Choline, a precursor of acetylcholine and phospholipids in the brain. *Progress in Brain Research*, 98, 197-200.
- Lorenz, M. D. (2011). *Handbook of Veterinary Neurology* (Fifth Edition). Elsevier, New York, Boston.
- Lorente de Nó R. (1934). Studies on the structure of the cerebral cortex. II. Continuation of the study of the ammonic system. *Journal of Psychology and Neurology*, 46, 113-177.
- Löscher, W. (1997). Animal models of intractable epilepsy. *Progress in Neurobiology*, 53(2), 239-258.

- Lothman, E. W., Stringer, J. L., Bertram, E. H. (1992). The dentate gyrus as a control point for seizures in the hippocampus and beyond. *Epilepsy Research. Supplement*, 7, 301-313.
- Martin-Vaquero, P., da Costa, R. C., Echandi, R. L., Sammet, C. L., Knopp, M. V., Sammet, S. (2012). Magnetic resonance spectroscopy of the canine brain at 3.0T and 7.0T. *Research in Veterinary Science*, 93(1), 427-429.
- Martlé, V., Ham, L. Van, Raedt, R., Vonck, K., Boon, P., Bhatti, S. (2014). Non-pharmacological treatment options for refractory epilepsy: An overview of human treatment modalities and their potential utility in dogs. *The Veterinary Journal*, 199, 332-339.
- Mathern, G. W., Babb, L., Pretorius, K. (1995). Reactive Synaptogenesis and Neuron Densities for Neuropeptide and Glutamate Decarboxylase Immunoreactivity in the Epileptogenic Human Fascia Dentata. *The Journal of Neuroscience*, 15(5 Pt 2), 3990-4004
- Mathews, P., Barker, P. B., Chatham, J. C., Bryan, R. N. (1995). Cerebral Metabolites in Patients with Acute and Subacute Strokes: by Q quantitative Proton. *American Journal of Roentgenology*, 165(3), 633-638.
- Maton, B., Londono, A., Sawrie, S. (2001). Postictal stability of proton magnetic resonance spectroscopy imaging (1H-MRSI) ratios in temporal lobe epilepsy. *Neurology*, 56, 251-253.
- Mehta, V., Namboodiri, M. A. (1995). N-acetylaspartate as an acetyl source in the nervous system. *Brain Research. Molecular Brain Research*, 31(1-2), 151-157.
- Mellema, L.M., Koblik, P. D., Kortz, G. D., LeCouteur, R. A., Chechowicz, M. A., Dickinson, P. J. (1999). Reversible magnetic resonance imaging abnormalities in dogs following seizures. *Veterinary Radiology & Ultrasound*, 40(6), 588-595.
- Mercimek-Mahmutoglu, S., Stoeckler-Ipsiroglu, S., Adami, A., Appleton, R., Araujo, H. C., Duran, M., Jakobs, C. (2006). GAMT deficiency: features, treatment, and outcome in an inborn error of creatine synthesis. *Neurology*, 67(3), 480-484.

- Miller, B. L., Chang, L., Booth, R., Ernst, T., Cornford, M., Nikas, D., Jenden, D. J. (1996). In vivo ¹H MRS Choline: Correlation with in vitro chemistry/histology. *Life Sciences*, 58(22), 1929-1935.
- Miller, S. P., Li, L. M., Cendes, F., Tasch, E. (2000). Medial temporal lobe neuronal damage in temporal and extratemporal lesional epilepsy. *Neurology*, 54, 1465-1470.
- Miyake, M., Kakimoto, Y., Sorimachi, M. (1981). A gas chromatographic method for the determination of N-acetyl-L-aspartic acid, N-acetyl-alpha-aspartylglutamic acid and beta-citryl-L-glutamic acid and their distributions in the brain and other organs of various species of animals. *Journal of Neurochemistry*, 36(3), 804-810.
- Mlynarik, V., Cudalbu, C., Xin, L., Gruetter, R. (2008). ¹H NMR spectroscopy of rat brain in vivo at 14.1 Tesla: Improvements in quantification of the neurochemical profile. *Journal of Magnetic Resonance*, 194(2), 163-168.
- Moffett, J. R., Arun, P., Ariyannur, P. S., Namboodiri, A. M. (2013). N-Acetylaspartate reductions in brain injury: Impact on post-injury neuroenergetics, lipid synthesis, and protein acetylation. *Frontiers in Neuroenergetics*, 5(12), 1-19.
- Moffett, J. R., Namboodiri, M. A. (1995). Differential distribution of N-acetylaspartylglutamate and N-acetylaspartate immunoreactivities in rat forebrain. *Journal of Neurocytology*, 24(6), 409-433.
- Moffett, J. R., Namboodiri, M. A., Neale, J. H. (1993). Enhanced carbodiimide fixation for immunohistochemistry: application to the comparative distributions of N-acetylaspartylglutamate and N-acetylaspartate immunoreactivities in rat brain. *The Journal of Histochemistry and Cytochemistry: Official Journal of the Histochemistry Society*, 41(4), 559-570.
- Moffett, J.R., Ross, B., Arun, P., Madhavarao, C. N., Namboodiri, A. M. (2007). N-Acetylaspartate in the CNS: from neurodiagnostics to neurobiology. *Progress in Neurobiology*, 81(2), 89-131.

- Montgomery, D. L., Lee, A. C. (1983). Brain Damage in the Epileptic Beagle Dog. *Veterinary Pathology*, 169, 160-169.
- Moreno, A., Ross, B. D., Blu, S. (2001). Direct determination of the N -acetyl- I - aspartate synthesis rate in the human brain by 13 C MRS and [1- 13C] glucose infusion, *Journal of Neurochemistry*, 77, 347-350.
- Mueller, S. G., Kollias, S. S., Trabesinger, A. H., Buck, A., Boesiger, P., Wieser, H. G. (2001). Proton magnetic resonance spectroscopy characteristics of a focal cortical dysgenesis during status epilepticus and in the interictal state. *Seizure*, 10(7), 518-524.
- Mueller, S. G., Laxer, K. D., Cashdollar, N. (2006). Spectroscopic evidence of hippocampal abnormalities in neocortical epilepsy. *European Journal of Neurology*, 13, 256-260.
- Muñana, K. R. (2013). Management of Refractory Epilepsy. *Topics in Companion Animal Medicine*, 28(2), 67-71.
- Munoz Maniega, S., Cvorovic, V., Chappell, F. M., Armitage, P. A., Marshall, I., Bastin, M. E., Wardlaw, J. M. (2008). Changes in NAA and lactate following ischemic stroke: a serial MR spectroscopic imaging study. *Neurology*, 71(24), 1993-1999.
- Nadler, J. V., Cooper, J. R. (1972). Metabolism of the aspartyl moiety of N-acetyl-L-aspartic acid in the rat brain. *Journal of Neurochemistry*, 19(9), 2091-2105.
- Neppl, R., Nguyen, C. M., Bowen, W., Al-Saadi, T., Pallagi, J., Morris, G., Rand, S. D. (2001). In vivo detection of postictal perturbations of cerebral metabolism by use of proton mr spectroscopy: Preliminary results in a canine model of prolonged generalized seizures. *American Journal of Neuroradiology*, 22(10), 1933-1943.
- Nickel R., Schummer A., Seiferle E., Verlag P. P. (2003). *Lehrbuch der Anatomie der Haustiere*, Band 5, Parey, Stuttgart.

- Nordahl, T. E., Salo, R., Natsuaki, Y., Galloway, G. P., Waters, C., Moore, C. D., Buonocore, M. H. (2005). Methamphetamine Users in Sustained Abstinence. *Archives of General Psychiatry*, 62(4), 444-52.
- Nyberg, S. L., Cerra, F. B., Gruetter, R. (1998). Brain lactate by magnetic resonance spectroscopy during fulminant hepatic failure in the dog. *Liver Transplantation and Surgery: Official Publication of the American Association for the Study of Liver Diseases and the International Liver Transplantation Society*, 4(2), 158-165.
- Ober, C. P., Warrington, C. D., Feeney, D. A., Jessen, C. R., Steward, S. (2013). Optimizing a protocol for 1H-magnetic resonance spectroscopy of the canine brain at 3T. *Veterinary Radiology and Ultrasound*, 54(2), 149-158.
- Ohtsuki, S., Tachikawa, M., Takanaga, H., Shimizu, H., Watanabe, M., Hosoya, K., Terasaki, T. (2002). The Blood–Brain Barrier Creatine Transporter is a Major Pathway for Supplying Creatine to the Brain. *Journal of Cerebral Blood Flow & Metabolism*, 22(11), 1327-1335.
- Olney, J. W., Price, M. T., Samson, L., & Labruyere, J. (1986). The role of specific ions in glutamate neurotoxicity. *Neuroscience Letters*, 65(1), 65-71.
- Ono, K., Kitagawa, M., Ito, D., Tanaka, N., Watari, T. (2014). Regional variations and age-related changes detected with magnetic resonance spectroscopy in the brain of healthy dogs. *American Journal of Veterinary Research*, 75(2), 179-186.
- Pakozdy A., Halasz P., Klang A., Bauer J., Leschnik M., Tichy A., Thalhammer J. G., Lang B., Vincent A. (2013). Suspected Limbic Encephalitis and Seizure in Cats Associated with Voltage-Gated Potassium Channel (VGKC) Complex Antibody. *Journal of Veterinary Internal Medicine*, 27(4), 982-984.
- Pakozdy, A., Gruber, A., Kneissl, S., Leschnik, M., Halasz, P., Thalhammer, J. G. (2011). Complex partial cluster seizures in cats with orofacial involvement. *Journal of Feline Medicine and Surgery*, 13(10), 687-693.

- Perasso, L., Cupello, A., Lunardi, G. L., Principato, C., Gandolfo, C., Balestrino, M. (2003). Kinetics of creatine in blood and brain after intraperitoneal injection in the rat. *Brain Research*, 974(1–2), 37-42.
- Petroff, O. A., Prichard, J. W., Behar, K. L., Alger, J. R., Shulman, R. G. (1984). In vivo phosphorus nuclear magnetic resonance spectroscopy in status epilepticus. *Annals of Neurology*, 16(2), 169-177.
- Pitkänen, A., Sutula, T. P. (2002). Is epilepsy a progressive disorder? Prospects for new therapeutic approaches in temporal-lobe epilepsy. *The Lancet Neurology*, 1(3), 173-183 .
- Podell, M., Hadjiconstantinou, M. (1997). Cerebrospinal fluid gamma-aminobutyric acid and glutamate values in dogs with epilepsy. *American Journal of Veterinary Research*, 58(5), 451-456.
- Ramon y Cajal S. (1893). Estructura del asta de Ammon y fascia dentata. *Anales de la Sociedad Española de Historia Natural*, 22, 53-114.
- Riederer, F., Bittsansky, M., Schmidt, C., Mlynarik, V., Baumgartner, C., Moser, E., Serles, W. (2006). 1H magnetic resonance spectroscopy at 3 T in cryptogenic and mesial temporal lobe epilepsy. *NMR in Biomedicine*, 19(5), 544-553.
- Rigotti, D. J., Inglese, M., Babb, J. S., Rovaris, M., Benedetti, B., Filippi, M., Gonen, O. (2007). Serial Whole-Brain N-Acetylaspartate Concentration in Healthy Young Adults. *American Journal of Neuroradiology*, 28(9), 1650-1651.
- Rincon, S. P., Blitstein, M. B., Caruso, P. A., González, R. G., Do, R. L., Ratai, E. (2016). The Use of Magnetic Resonance Spectroscopy in the Evaluation of Pediatric Patients With Seizures. *Pediatric Neurology*, 58, 57-66.
- Risio, L. De, Bhatti, S., Muñana, K., Penderis, J., Stein, V., Tipold, A., Packer, R. M. A. (2015). International veterinary epilepsy task force consensus proposal: diagnostic approach to epilepsy in dogs. *BMC Veterinary Research*, 11, 148.
- Rosenberg, E. H., Almeida, L. S., Kleefstra, T., de Grauw, R. S., Yntema, H. G., Bahi, N., Salomons, G. S. (2004). High prevalence of SLC6A8 deficiency in X-linked mental retardation. *American Journal of Human Genetics*, 75(1), 97-105.

- Roy, S., Nicholson, D. W. (2000). Cross-talk in cell death signaling. *The Journal of Experimental Medicine*, 192(8), 21-5.
- Rusbridge, C., Long, S., Jovanovik, J., Milne, M., Berendt, M., Bhatti, S. F., Volk, H. A. (2015). International Veterinary Epilepsy Task Force recommendations for a veterinary epilepsy-specific MRI protocol. *BMC Veterinary Research*, 11(1), 194.
- Sander, J. W. A. S. (1993). Some Aspects of Prognosis in the Epilepsies: A Review. *Epilepsia*, 34(6), 1007-1016.
- Savic, I., Lekvall, A., Greitz, D., Helms, G. (2000). MR spectroscopy shows reduced frontal lobe concentrations of N-acetyl aspartate in patients with juvenile myoclonic epilepsy. *Epilepsia*, 41(3), 290-296.
- Savic, I., Österman, Y., Helms, G. (2004). MRS shows syndrome differentiated metabolite changes in human-generalized epilepsies. *NeuroImage*, 21(1), 163-172.
- Schmidt, M. J., Kramer, M. (2015), MRT-Atlas ZNS-Befunde bei Hund und Katze . Enke Verlag, Stuttgart.
- Schulze, A., Hess, T., Wevers, R., Mayatepek, E., Bachert, P., Marescau, B., Rating, D. (1997). Creatine deficiency syndrome caused by guanidinoacetate methyltransferase deficiency: diagnostic tools for a new inborn error of metabolism. *The Journal of Pediatrics*, 131(4), 626-631.
- Seppälä, E. H., Jokinen, T. S., Fukata, M., Fukata, Y., Webster, M. T., Karlsson, E. K., Lohi, H. (2011). Lgi2 truncation causes a remitting focal epilepsy in dogs. *PLoS Genetics*, 7(7).
- Simister, R. J., McLean, M. A., Barker, G. J., Duncan, J. S. (2003). A proton magnetic resonance spectroscopy study of metabolites in the occipital lobes in epilepsy. *Epilepsia*, 44(4), 550-558.

- Sloviter, R. S. (2008). Hippocampal epileptogenesis in animal models of mesial temporal lobe epilepsy with hippocampal sclerosis: The importance of the "latent period" and other concepts. *Epilepsia*, 49(9), 85-92.
- Sommer W. (1880). Erkrankung des Ammonshornes als aetiologisches Moment der Epilepsie. *Archiv für Psychiatrie und Nervenkrankheiten*, 361-375.
- Spencer, S. S., Marks, D., Katz, A., Kim, J., Spencer, D. D. (1992). Anatomic correlates of interhippocampal seizure propagation time. *Epilepsia*, 33(5), 862-873.
- Spencer, S. S., McCarthy, G., Spencer, D. D. (1993). Diagnosis of medial temporal lobe seizure onset: relative specificity and sensitivity of quantitative MRI. *Neurology*, 43(10), 2117-2124.
- Spruston, N., Mcbain, C. J. (2007). The Hippocampus Book. *Structural and Functional Properties of Hippocampal Neurons*, 133-201.
- Stagg, C. J., Rothman, D. L. (2013). Magnetic Resonance Spectroscopy: Tools for Neuroscience Research and Emerging Clinical Applications. Elsevier, Oxford UK.
- Steen, C., Wilczak, N., Hoogduin, J. M., Koch, M., de Keyser, J. (2010). Reduced creatine kinase B activity in multiple sclerosis normal appearing white matter. *PLoS ONE*, 5(5).
- Stockler, S., Schutz, P. W., Salomons, G. S. (2007). Cerebral creatine deficiency syndromes: clinical aspects, treatment and pathophysiology. *Sub-Cellular Biochemistry*, 46, 149-166.
- Suhy, J., Rooney, W. D., Goodkin, D. E., Capizzano, A. A., Soher, B. J., Maudsley, A. A., Weiner, M. W. (2000). 1H MRSI comparison of white matter and lesions in primary progressive and relapsing-remitting MS. *Multiple Sclerosis*, 6(3), 148-155.

- Tartaglia, M. C., Narayanan, S., De Stefano, N., Arnaoutelis, R., Antel, S. B., Francis, S. J., Arnold, D. L. (2002). Choline is increased in pre-lesional normal appearing white matter in multiple sclerosis. *Journal of Neurology*, 249(10), 1382-1390.
- Thom, M. (2009). Hippocampal Sclerosis: Progress Since Sommer. *Brain Pathology*, 19(2), 565-572.
- Vullo, T., Deo-Narine, V., Stallmeyer, B. M., Gomez, P. T. (1996). Quantification of normal canine hippocampus formation volume: Correlation of MRI with gross histology. *Magnetic Resonance Imaging*, 14(6), 657-662.
- Thomas, W. B. (2010). Idiopathic epilepsy in dogs and cats. *The Veterinary Clinics of North America. Small Animal Practice*, 40(1), 161-179.
- Uemura, E. E. (2015). *Fundamentals of Canine Neuroanatomy and Neurophysiology*. Wiley Blackwell, New Jersey.
- Urenjak, J., Williams, S. R., Gadian, D. G., Noble, M. (1992). Specific Expression of N-Acetylaspartate in Neurons, Oligodendrocyte-Type-2 Astrocyte Progenitors, and Immature Oligodendrocytes In Vitro. *Journal of Neurochemistry*, 59(1), 55-61.
- Valenzuela, M.J., Sachdev, P. (2001). Magnetic resonance spectroscopy in AD. *Neurology*, 56(5), 592-598.
- Van der Knaap, M. S., Van Der Voorn, P., Barkhof, F., Van Coster, R., Krägeloh-Mann, I., Feigenbaum, A., Pouwels, P. J. W. (2003). A new leukodystrophy with brainstem and spinal cord involvement and high lactate. *Annals of Neurology*, 53(2), 252-258.
- Vermathen, P., Ende, G., Laxer, K. D., Walker, J. A., Knowlton, R. C., Barbaro, N. M., Weiner, M.W. (2002). Temporal lobectomy for epilepsy: recovery of the contralateral hippocampus measured by (1)H MRS. *Neurology*, 59(4), 633-636.

- Vezzani, A., Conti, M., De Luigi, A., Ravizza, T., Moneta, D., Marchesi, F., De Simoni, M. G. (1999). Interleukin-1beta immunoreactivity and microglia are enhanced in the rat hippocampus by focal kainate application: functional evidence for enhancement of electrographic seizures. *The Journal of Neuroscience: The Official Journal of the Society for Neuroscience*, 19(12), 5054-5065.
- Volk, H. A. (2015). International Veterinary Epilepsy Task Force consensus reports on epilepsy definition, classification and terminology, affected dog breeds, diagnosis, treatment, outcome measures of therapeutic trials, neuroimaging and neuropathology in companion animals. *BMC Veterinary Research*, 11(1), 174.
- Wagner, E., Rosati, M., Molin, J., Foitzik, U., Wahle, A. M., Fischer, A., Matiasek, K. (2014). Hippocampal sclerosis in feline epilepsy. *Brain Pathology*, 24(6), 607-619.
- Warrington, C. D., Feeney, D. A., Ober, C. P., Jessen, C. R., Steward, S. M., Armién, A. G. (2013). Relative metabolite concentrations and ratios determined by use of 3-T region-specific proton magnetic resonance spectroscopy of the brain of healthy Beagles. *American Journal of Veterinary Research*, 74(10), 1291-1303.
- Williamson, P. D., Thadani, V. M., French, J. A., Darcey, T. M., Mattson, R. H., Spencer, S. S., Spencer, D. D. (1998). Medial temporal lobe epilepsy: videotape analysis of objective clinical seizure characteristics. *Epilepsia*, 39(11), 1182-1188.
- Woermann, F. G., McLean, M. A., Bartlett, P. A., Parker, G., Barker, G. J., Duncan, J. S. (1999). Short echo time single-voxel 1H magnetic resonance spectroscopy in magnetic resonance imaging-negative temporal lobe epilepsy: different biochemical profile compared with hippocampal sclerosis. *Annals of Neurology*, 45(3), 369-376.
- Wong, R. K., Watkins, D. J. (1982). Cellular factors influencing GABA response in hippocampal pyramidal cells. *Journal of Neurophysiology*, 48(4), 938-951.

Wrzosek, M., Podgórski, P., Drobot, P., Bodys, W., Nicpoń, J. (2016). The MR Volumetric Brain Assessment in Canine Epileptic Patient - A Pilot Study, oral presentation at the 29th Symposium of the ESVN- ECVN Edinburgh, United Kingdom.

Yaffe, K., Ferriero, D., Barkovich, A. J., Rowley, H. (1995). Reversible MRI abnormalities following seizures. *Neurology*, 45(1), 104-108.

Yamasaki, H., Uruoka, H. F., Kechi, M. A., Itakura, C. (1991). Neuronal Loss and Gliosis in Limbic System in an Epileptic Dog. *Veterinary Pathology*, 78(2-3), 540-542.

9. Ethics

The study was performed in the Department of Internal Medicine with a Clinic of Horses, Dogs and Cats, Faculty of Veterinary Medicine, Wrocław University of Environmental and Life Sciences, Wrocław, Poland. The study was conducted according to the University Wrocław's institutional guidelines. According to the Polish law, approval from the Ethical Committee was not required as all examinations were performed for diagnostic reasons at the owner's request (Experiments on Animals Act from January 15, 2015, *Journal of Laws of the Republic of Poland* from 2015, item. 266). Informed owner consent was obtained for the dogs to be eligible for enrolment into this study.

Erklärung

Ich erkläre: „Ich habe die vorgelegte Dissertation selbstständig und ohne unerlaubte fremde Hilfe und nur mit den Hilfen angefertigt, die ich in der Dissertation angegeben habe. Alle Textstellen, die wörtlich oder sinngemäß aus veröffentlichten oder nicht veröffentlichten Schriften entnommen sind, und alle Angaben, die auf mündlichen Auskünften beruhen, sind als solche kenntlich gemacht. Bei den von mir durchgeführten und in der Dissertation erwähnten Untersuchungen habe ich die Grundsätze guter wissenschaftlicher Praxis, wie sie in der „Satzung der Justus-Liebig-Universität Gießen zur Sicherung guter wissenschaftlicher Praxis“ niedergelegt sind, eingehalten.“

Agnieszka Olszewska



édition scientifique
VVB LAUFERSWEILER VERLAG

VVB LAUFERSWEILER VERLAG
STAUFENBERGRING 15
D-35396 GIESSEN

Tel: 0641-5599888 Fax: -5599890
redaktion@doktorverlag.de
www.doktorverlag.de

ISBN: 978-3-8359-6765-6

